UNIVERSITY OF CALIFORNIA
Santa Barbara

Experimental apparatus for the study of Faraday waves on time-varying domains

A thesis submitted in partial satisfaction
of the requirements for the degree of

Master of Science

in

Mechanical Engineering

by

Rory E. Hartong-Redden

Committee in Charge:

Professor Rouslan Krechetnikov, Co-Chair

Professor Jeff Moehlis, Co-Chair

Professor Ted Bennett

December 2014

The thesis of
Rory E. Hartong-Redden is approved:

Professor Ted Bennett

Professor Jeff Moehlis, Committee Co-Chairperson

Professor Rouslan Krechetnikov, Committee Co-Chairperson

September 2014

Experimental apparatus for the study of Faraday waves on time-varying domains

by

Rory E. Hartong-Redden

Acknowledgements

I want to thank Ted Bennett, Jeff Moehlis, Rouslan Krechetnikov, Hans Mayer and Andy Weinberg.

Abstract

Experimental apparatus for the study of Faraday waves on time-varying domains

Rory E. Hartong-Redden

A variation of a classical fluid dynamics experiment on Faraday waves is motivated by interest in understanding pattern formation on time-dependent domains. In the classical studies, a fluid layer when vibrated vertically will generate standing waves known as Faraday waves. To investigate the effect of a time-varying domain on Faraday waves, a vibrating fluid container with dimensions which can be controlled in a time-dependent fashion was designed and constructed. This thesis covers the design of an experimental apparatus and the application of a measurement technique for use in future studies.

Contents

List of Figures

List of Tables

Chapter 1

Physical motivation

It is often the case that experiments motivate theory. After Michael Faraday's discovery of his namesake phenomena in 1831 [1] it was over 100 years until a convincing theoretical explanation was given [2]. Only recently was this classical problem considered solved when experiments [3] found good agreement with theory [4].

Over the decades of modern science Faraday waves were used as a testbed for new physics and paradigms. In the 1980s when Chaos was in fashion, studies focused on Faraday waves as a model for chaotic dynamics [5]. Starting in the 1990s, more powerful digital cameras and computers enabled broader studies of the phase space of Faraday waves and with it an understanding of the complex symmetries found in Faraday wave patterns [6, 7].

Along these lines, this investigation focuses on the role of the domain in determining Faraday waves patterns. The waves exist on a domain, typically a cylin-

drical container, but no study has considered varying the size of the container in real-time while observing the effect on the resultant waves. Theoretical tools are being developed [8] to treat problems with time-dependent domains, which also find application in other numerous areas such as biological stripes, chemistry, metallurgy and fluid dynamics.

Any physical problem comprises a governing equation and a set of boundary conditions. Early experiments sought to disentangle the role of the boundary conditions from the physics in the bulk of the fluid and many experiments framed domain effects as a hindrance in their observation of Faraday waves [9]. Simonelli and Gollub [10] were the first to focus on the geometry of boundary conditions of Faraday waves when they compared patterns in a square container with those in slightly non-square (rectangular) container. Another experimental variation investigated the time-dependence of the forcing by extending the forcing from one to two frequencies [6].

The proposed experiment will investigate how a time-varying domain affects the Faraday wave patterns. To that end, the experiment must produce Faraday waves (a non-trivial task in itself), time-dependently change the container dimensions, and measure the characteristics of the resultant patterns.

Chapter 2

Identifying requirements for setup

This chapter introduces important aspects of Faraday waves and looks at the published literature as a guide for the development of this experiment. The motivating research interest is translated into engineering design targets.

2.1 Faraday waves

When a container is filled with a liquid, typically water or oil, and vibrated sufficiently forcefully in the direction of gravity, surface waves are generated as in Figure 2.1. A shaking container may generate capillary waves due to motion of the contact line; these waves travel from the outer edge of the container inward. Emerging in the center of the fluid are standing waves which are generated from another source. These waves owe their existence to an instability of vibrating fluid

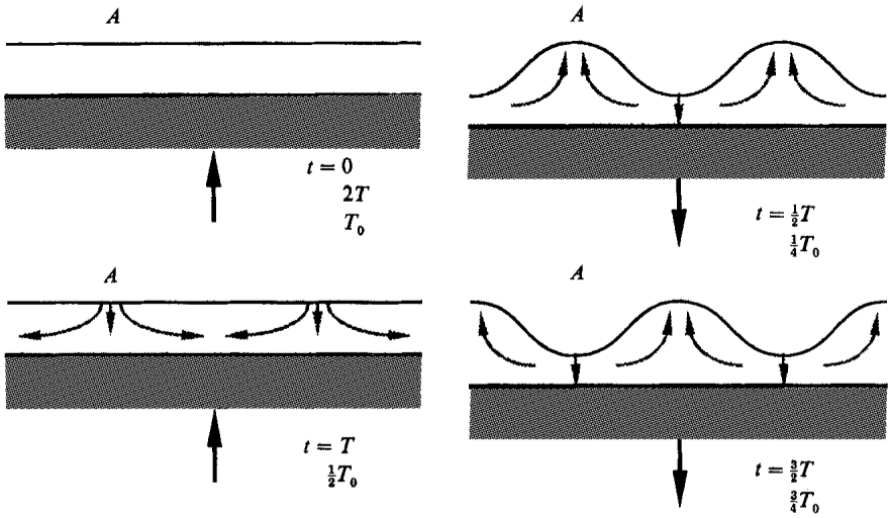

Figure 2.1: A simplified physical picture of Faraday waves [9] illustrating why the Faraday wave period T_0 is twice the driving period T, $T_0 = 2\,T$.

and are called Faraday waves. Seen from above, the waves have patterns with a large variety of shapes and symmetries depending on the fluid properties, depth, driving conditions, and sometimes the boundary conditions.

A simplified physical picture of the waves is presented in Figure 2.1. As the container accelerates upward the fluid interface is destabilized and deforms. When an up-down cycle is completed, the surface returns to the flat state but inertia carries the maxima into the minima, inverting the waves. As a result, Faraday waves oscillate at half the forcing frequency.

2.1.1 Dispersion relation

Some additional insight into the physics of Faraday waves is gained by taking a mathematical approach. The first successful treatment was a linear stability analysis of an inviscid fluid, which showed that the origin of the waves is a parametric resonance and that the amplitude of the waves obeys the Mathieu equation [2]. A common example of parametric resonance is kicking your legs on a swing to go higher. Faraday waves are often called parametric resonance waves in recognition of their origin.

Following [11, 2] and without going into too much detail, we retrace the analysis of Faraday waves. Consider again Figure 2.1 with a fluid of depth h with interface $z = \zeta(x, y, t)$. The interface is expanded into Fourier modes $\zeta_{\mathbf{k}}(t)$,

$$\zeta(x, y, t) = \int_{-\infty}^{\infty} \mathrm{d}\mathbf{k}\, \zeta_{\mathbf{k}}(t) e^{i\mathbf{k}\cdot\mathbf{r}}\,. \tag{2.1}$$

For an inviscid fluid, taking into account surface tension and gravity and neglecting nonlinear terms in surface deformation and boundary effects, we find that each eigenmode $\zeta_{\mathbf{k}}(t)$ obeys the Mathieu equation

$$\ddot{\zeta}_{\mathbf{k}} + \omega_0^2(t)\zeta_{\mathbf{k}} = 0\,, \tag{2.2}$$

where the natural frequency $\omega_0(t)$ of each mode is found from the dispersion relation

$$\omega_0^2(t) = \tanh(kh)\left(g(t)k + \frac{\gamma}{\rho}k^3\right)\,. \tag{2.3}$$

Time-dependence enters through an imposed gravitational oscillation $g(t) = g - a\cos(\omega t)$, in the frame of the moving fluid, and the condition for parametric resonance is when the natural frequency ω_0 is half the driving frequency ω, $\omega_0 = \omega/2$. The excited wavelength, then, is governed by this inviscid dispersion relation for surface waves of depth h, wavenumber $k = 2\pi/\lambda$, angular driving frequency ω, and surface tension γ. Often the pattern size is smaller than the fluid depth, $kh > 3$, so that the infinite depth approximation $\tanh(kh) = 1$ can be invoked.

There are two competing forces in Equation (2.3). The gravitational term balances the capillary term when

$$k = \sqrt{\frac{\rho g}{\gamma}}\,. \tag{2.4}$$

For clean water, $\gamma = 72$ dyne/cm, the forces balance at the capillary length, $\lambda_c \sim 1/k = 2.7$ mm. The capillary length is also the length scale of ripples which imposes the resolution requirement discussed in §2.3.

2.1.2 Threshold acceleration

After the initial success with the inviscid analysis, attention turned in the early 1990s to incorporating viscosity and to predicting the minimum acceleration or threshold acceleration for which Faraday waves form [11]. In the infinite depth

approximation and the capillary regime, the threshold acceleration a_c is [6]

$$a_c = 8 \left(\frac{\rho}{\gamma} \right)^{1/3} \nu \, \omega^{5/3} \, . \tag{2.5}$$

A few results for a_c follow:

- dependence on the surface tension and density is weak,
- acceleration threshold scales with viscosity,
- threshold increases quickest with frequency.

Equation (2.5) provides broad insights useful for designing an experiment. Given the linear dependence on viscosity, an experiment probing high acceleration thresholds may prefer a viscous silicon oil to water in order to keep the driving frequencies low. The maximum forcing acceleration, determined by the driven mass and force output, sets the highest achievable wave frequency, from Equation (2.5), and consequently the smallest pattern size, from Equation (2.3).

2.2 Size of experiment

As mentioned above, the total mass of the system and the peak force of the shaker determine the maximum achievable acceleration of the system. However, vibration systems increase exponentially in cost as the rated force increases from 10 N to 10 kN and higher. When the size of the experiment increases so does its weight which in turn requires a more expensive vibration system. The appropriate

Authors	Size (cm)	Depth (cm)	Kinematic viscosity (cm^2/s)	Surface tension (dyne/cm)	Driving frequency (Hz)
Benjamin and Ursell [2]	Ø 5.4	25	0.01	72	16
Ciliberto and Gollub [5]	Ø 12.7	1	0.01	72	15–17
Douady and Fauve [12]	8.06 x 8.06	0.5	-	-	-
Simonelli and Gollub [10]	6 x 6	2.5	0.03	24	12
Douady [9]	6.5 x 1.6	0.5	0.01	29.5	20–30
Edwards and Fauve [6]	Ø 12	0.29	1.00	65	
Bechhoefer et al. [11]	Ø 10, 11.4 x 11.4	1.0, 0.7, 0.24	0.5–2	26–30	20–80
Lioubashevski [13]	Ø 14.40	0.1–0.3	0.4 - 1.7	29.6–31.0	20–80
Binks and van de Water [14]	Ø 44.0	2.0	0.034	18.3	25–45
Shats et al. [15]	Ø 17.8	3.0	0.01	73	10–200

Table 2.1: Experimental parameters for a number of notable Faraday wave experiments arranged by publication date. For comparison, pure water has a surface tension value of 72 dyne/cm (mN/m) and viscosity of 0.01 cm^2/s. The viscosity of oils are often varied with temperature, producing a range of experimental values.

system size, even given a choice of working fluid, was an important consideration; to this end, it is useful to consider what length scale was used in previous experiments. Table 2.1 illustrates the range of experimental length scales along with the working fluid properties in a number of Faraday wave experiments. Many experiments use circular geometries about 12 cm in diameter (Ø) with water as the working fluid.

It is often mentioned by experimenters that the ideal depth is in the infinite depth regime, with a fluid depth larger than the nominal excited wavelength, but shallow enough to damp long wavelength modes [11]. In practice this translates to

0.1–1 cm but at high enough driving frequency the pattern size becomes smaller than any given fluid depth which can then be considered infinite.

2.3 Design requirements

Summarizing the above discussion, we arrive at the following design requirements for a Faraday wave experiment. First and foremost, the vertical motion must be in the regime where Faraday waves are generated. For a variety of working fluids over a span of viscosities, we set a goal for the vertical actuator to generate up to 10 g (100 m/s^2) at a frequency up to 500 Hz.

In addition to the vertical motion, the horizontal motion must modulate the container size. The requirements here are low-level acceleration, or no acceleration for constant motion in the mm/s range, which does not disrupt the oscillating Faraday waves.

To quantitatively study the Faraday waves, we seek to measure the fluid interface $z = h(x, y, t)$ with the appropriate spatial and temporal resolution. The spatial resolution is dictated by the smallest feature of interest, the capillary length, which is about 3 mm for water. Furthermore, this resolution must hold across the entire fluid interface. The sampling frequency should be at the drive frequency, or twice the natural frequency of the standing waves, up to 100 Hz.

Parameter	Design goal	Comments
Container size	15 cm x 15 cm	Length by width
Container depth	1.27 cm (0.5 in)	Typical fluid depth is 1 cm
Horizontal frequency	0–0.5 Hz	Cycle frequency
Horizontal amplitude	0–0.3 g	Acceleration
Horizontal speed	0–20 mm/s	Constant speed motion
Vertical frequency	5–500 Hz	Sinusoidal motion
Vertical amplitude	0–10 g	Acceleration
Measurement frequency	100 Hz	Sample rate
Measurement resolution	3 mm	Lateral (x, y) and height (z)
Measurement area	300 cm^2	Sample area

Table 2.2: The requirements for the experimental apparatus and measurement system are summarized with these design goals.

Chapter 3

Engineering design

This chapter describes the scope of the Faraday wave experiment and the underpinning engineering design. Section 3.1 is an overview of the experiment which is then described in more detail in the following sections. The operational details are left for the appendix §A.

3.1 Overview

The basic idea for the experiment is given in Figure 3.1. Faraday Waves are generated by imposing a sufficiently large vertical acceleration $g(t)$. To vary the domain size in time, the container dimensions are modulated using two independent sidewalls moving in the horizontal direction. The container consists of four walls, two which are fixed and two which are free to move linearly, and a transparent bottom. We study the fluid interface inside this container, ignoring fluid outside this defined space. To keep the fluid depth constant in the container

the moving walls do not reach the bottom of the container, allowing flow underneath the wall. While the two sidewall locations, x_1 and x_2 from Figure 3.1, can be controlled independently the rest of the experiment as implemented assumes $x_1 = -x_2$, i.e. they move symmetrically with respect to the centerline of the container.

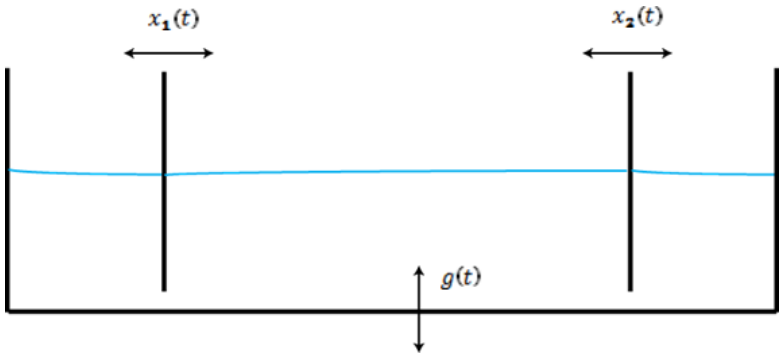

Figure 3.1: Schematic showing a side view of the rectangular container with two moving walls on the left and right; the entire container moves vertically in time according to acceleration $g(t)$.

The experiment allows $g(t)$ to be an arbitrary bounded function. The variation of driving acceleration was not investigated and we take the canonical function in these experiments where $g(t)$ is a sine wave:

$$g(t) = a \sin(2\pi f_v t)\,. \tag{3.1}$$

The frequency f_v is arbitrary as well, in practice we take $f_v \sim 20$ Hz.

The left and right walls can be freely moved along one dimension. For simplicity, we vary the area of the domain linearly and the walls move with constant

speed,

$$\dot{x}_1(t) = \pm v\,, \tag{3.2}$$

going forward and backward for equal durations over a period T. Considering that moving the walls x_1 and x_2 quickly generates waves which can overwhelm the Faraday waves, the time scale of horizontal motion is necessarily larger than that of the vertical motion. The frequency of the prescribed horizontal motion cycle is two orders of magnitude less than the vertical motion and $f_h = 1/T \sim 0.1$ Hz.

3.2 Components

The design components are classified according to their function. The optics system is a separate structure, apart from the Faraday apparatus in Figure 3.2, which images and measures the Faraday waves. Table 3.1 lists the main components — which each function independently — as horizontal actuators, vertical transducers, optics, or the mechanical structure.

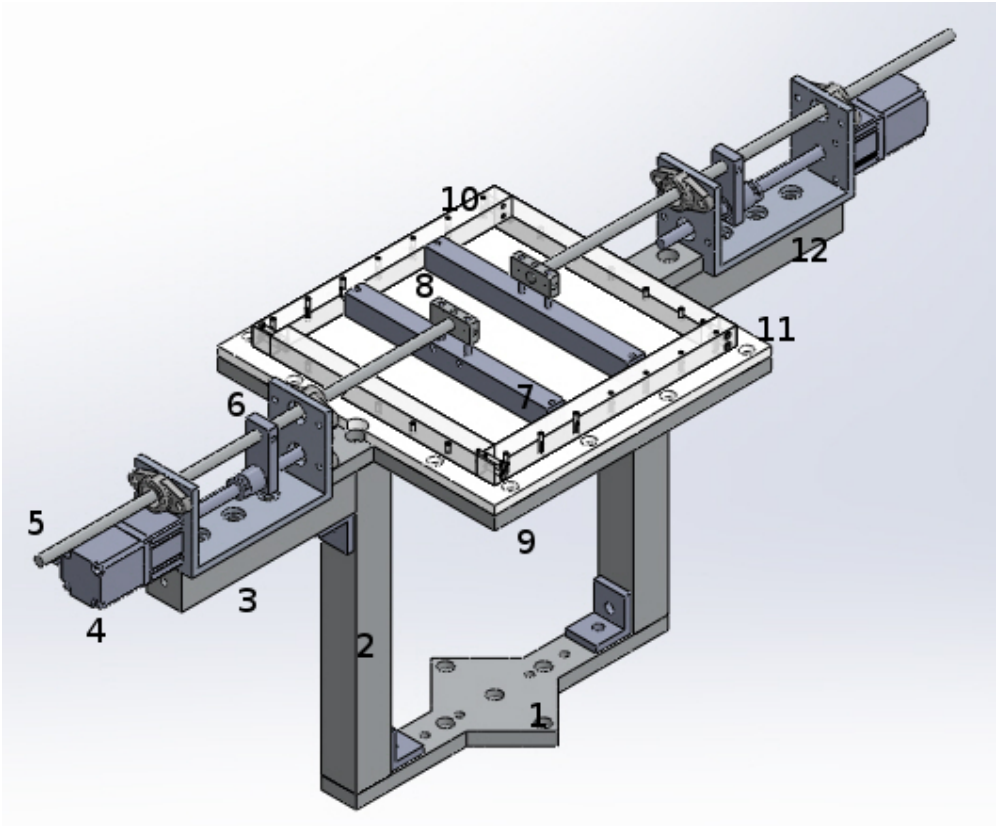

Figure 3.2: The Faraday assembly rendered here was designed using CAD software. The main parts of the assembly are labeled by number: (1) base plate, (2) vertical column, (3) horizontal column, (4) stepper motor, (5) shaft, (6) traveling nut connector, (7) moving wall, (8) wall connector, (9) container support rim, (10) parallel container walls, (11) container bottom (on top of #9), (12) U-Channel.

Components	Function
Camera Projector Mirrors Vertical stages	Optics
Stepper motors Moving walls Controllers Computer program	Horizontal actuators
Shaker Accelerometers LabVIEW	Vertical transducers
Base plate Vertical pillars Horizontal beams Container support rim U-Channel	Mechanical structure

Table 3.1: Different components of the design function independently on top of the mechanical structure.

3.3 Vertical motion

The vertical accelerations which generate Faraday waves require relatively large forces (300 N) fluctuating on small timescales (100 μs). From a design point of view, small voicecoil actuators are sufficiently responsive but not forceful enough while electric motors can be very powerful but lack responsiveness. An actuator with these characteristics is an audio amplifier and speaker system, a vibration system.

The system consists of a high quality speaker (shaker) and amplifier (linear amplifier). Referring to Figure 3.4, the path for the driving acceleration signal

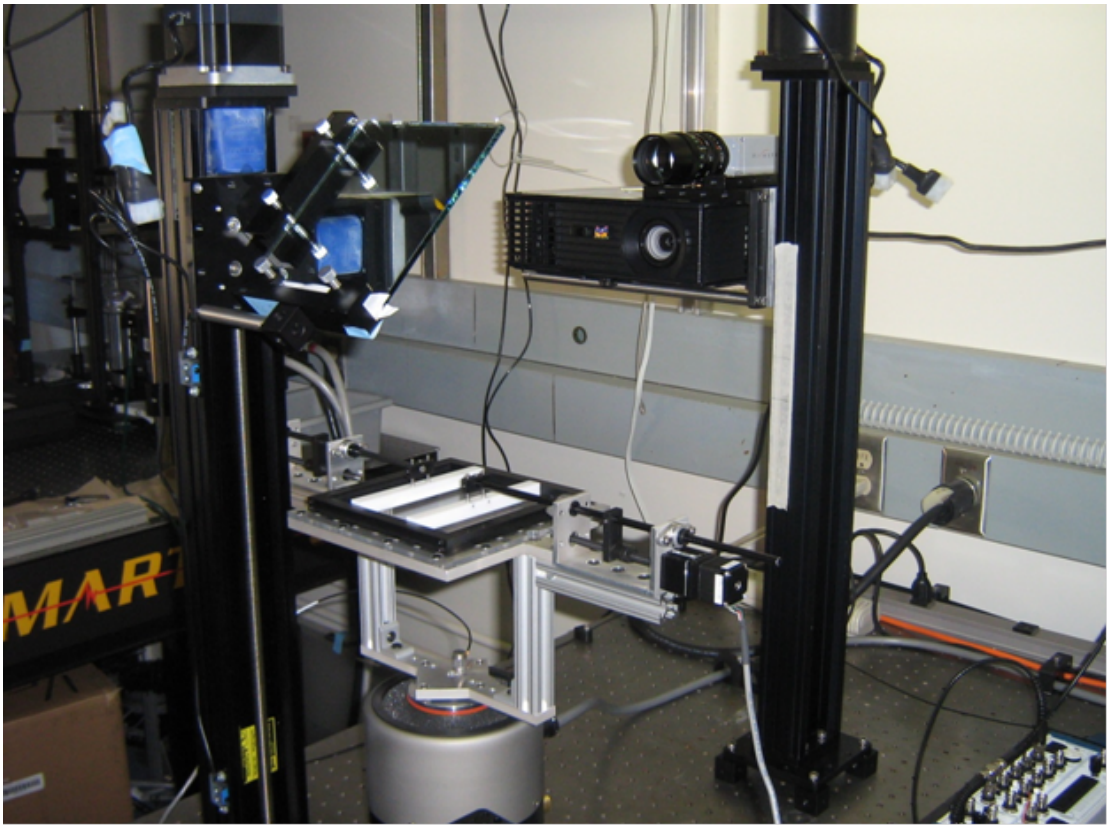

Figure 3.3: Fully assembled experimental setup: shaker (bottom center), container with linear actuators (middle), mirror mounted to vertical stage, video camera atop video projector on vertical stage (right), at the bottom right is the DAQ.

begins with the PC where a LabVIEW Virtual Instrument which generates a digital signal, the signal is converted to an analog voltage by the Data Acquisition Device (DAQ), the voltage is then amplified to drive the shaker. An accelerometer, interfacing with a signal conditioner, sends the measured signal to an oscilloscope and DAQ for readout.

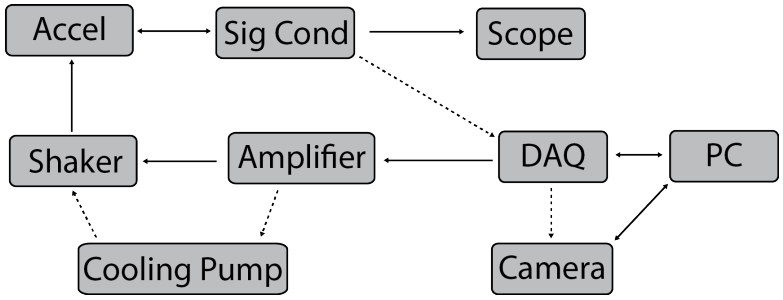

Figure 3.4: Shown is a system chart of components used to produce and measure vertical motion. Arrows indicate the direction of the flow of information, e.g. from the sensor to computer, and dashed arrows indicate possible future connections.

In a fully-functional system the PC will control each of the experimental functions and communicate with the shaker, signal conditioner and camera. This unified control will enable the synchronization of the images with the acceleration measurement as well as location of the moving walls; when each system is operated individually without a common reference, the time-stamps on the data do not correspond.

3.3.1 Vibration system

The Labworks LB–139.141–75 is a vibration test system similar to an audio system in the sense that like audio systems it contains a speaker and amplifier with the addition a cooling blower. Vibration systems are typically used in vibration testing where any number of driving forces such as impulsive, sinusoidal, or random can be applied to test a system.

The shaker is the speaker component of the system where a permanent magnet and surrounding coils convert electrical current into mechanical motion. The linearity of the system allows simple and effective open-loop control.

In sinusoidal motion, the shaker is limited by frequency and amplitude. The frequency response of the shaker is 0–6,500 Hz which is limited on the upper end by the resonance frequency of the shaker. The maximum payload is 7 lbs (3.2 kg) and with decreasing payload the peak acceleration increases: 13 g peak with 5 lb load and 38 g with 1 lb. At high frequencies the amplitude limitation is imposed by the 75 lb peak force but at low frequencies the limitation is due to the maximum displacement of 1 inch peak-to-peak. Therefore, the lower working limit of the shaker is 5 Hz.

The shaker is sensitive to the center of mass of the load. That is, the shaker is only designed to provide a uniaxial force so the center of mass of the load is ideally located on the central axis of the shaker. Side-to-side motion not only is an unwanted noise but can damage the delicate shaker. Therefore, it is important that the Faraday apparatus mounted on top of the shaker maintain a constant center of mass.

3.3.2 Computer interface

An important design consideration was that all components interface with a computer. When the driving signal is generated digitally any functional form is possible whereas an analog function generator limits output to a handful of predefined forms.

We chose a data acquisition system (DAQ) from National Instruments (NI). The main requirements of the DAQ is that it has a 100 kHz sample rate or higher and multiple analog input and outputs. We chose a DAQ based on the PCI express platform, the NI PCIe-6363, with 32 analog inputs sampled at 2 million samples per second (MS/s) and 4 analog outputs sampled at 2.86 MS/s. The DAQ is more than adequate for the demands of 100 Hz signals we expect in this experiment. One analog output is dedicated to the driving signal for the linear amplifier and two analog inputs are required for the pair of accelerometers. Additional inputs and outputs enable future functions to be incorporated into the existing setup.

3.3.3 Accelerometers

Accelerometers are used to measure the level of forcing applied the fluid. Two Brüel and Kjær Type 4513 accelerometers were chosen because they come with a factory-provided calibration and accuracy of 1%. The pair of accelerometers are each powered by a Type 1704-A-001 signal conditioner which also amplifies the

signal for the DAQ or oscilloscope. The primary accelerometer, aligned vertically, measures the amplitude of the forcing acceleration. The second accelerometer is mounted horizontally to measure the off-axis acceleration, or noise. The signal conditioners amplify the accelerometer output to a range appropriate for the DAQ, ± 5 V.

3.4 Horizontal motion

Two horizontal linear actuators position two sliding walls which vary the size of the container in one dimension. The horizontal actuators in Figure 3.6 mounted on the Faraday apparatus which is fastened to the shaker at the base. The leadscrew, nut, nut connector, shaft, wall connector, sliding wall, and stepper motor comprise a linear actuator which converts the rotatory motion of the stepper motor into linear motion.

The mass and center of mass of the horizontal actuators were key considerations because they are driven by the shaker along with the rest of the Faraday apparatus. As seen in figure 3.6, symmetrically opposing motion of walls keeps the center of mass located over the center of the shaker. To reduce the load on the shaker, the actuators are simple, light, and stiff, weighing less than 1 kg each.

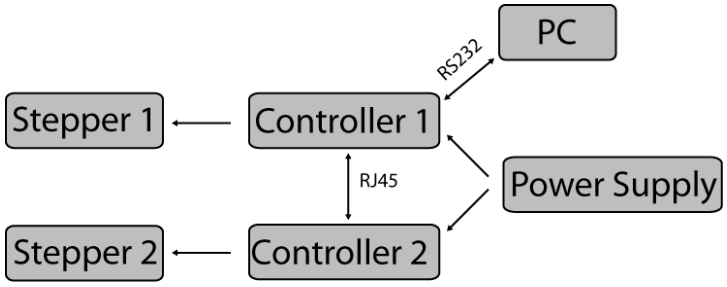

Figure 3.5: A power supply provides power to both controllers, one of which is connected to a computer which then communicates with the second controller. Each controller drives a single stepper motor without feedback.

Tracing the flow chart in figure 3.5, the path of the control signal originates with the PC, as with the vertical system. The signal goes from the PC to a pair of controllers where each drives a stepper motor actuating a moving wall.

3.4.1 Linear actuators

The requirements of low mass forced the design to a simple linear actuator setup. The Parker LD28 stepper motor and leadscrew system was chosen for its low mass: 0.6 kg including a leadscrew allowing 12 cm of travel. With the leadscrew and nut a simple, stiff, lightweight linear actuator design arose. As a compromise between speed and accuracy, the nut is threaded at 3 mm/revolution which enables the nut to travel between 0 and 45 mm/s, the nominal speed is 1 mm/s. The small NEMA 11 motor has a peak torque of 0.06 Nm so the traveling nut can accelerate up to 2 g (20 m/s^2).

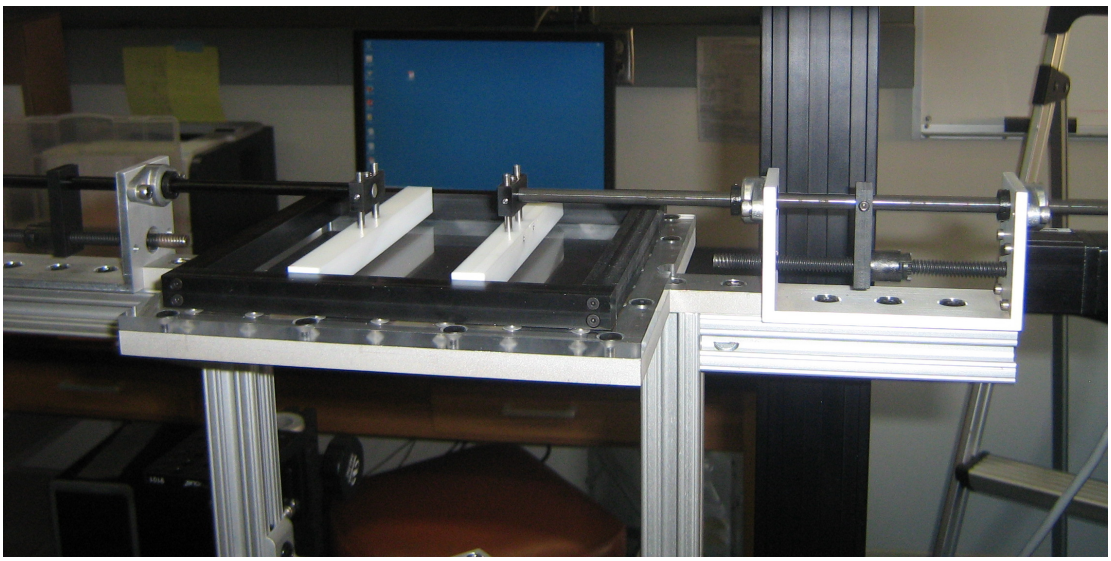

Figure 3.6: Two horizontal linear actuators position two sliding walls. The actuator on the right is described from right to left: the stepper motor and leadscrew is attached to the end of the u-channel, the threaded nut moves along the leadscrew, the nut connector fastens to the shaft which slides in two linear bearings, the wall connector at the end of the shaft fastens to the Teflon sliding wall.

Each traveling nut is connected to a sliding wall. Two sets of walls were made of Delrin and Teflon. The latter was chosen for its lubricating properties and ability to slide inside the outer container walls. The moving walls and actuators provide unimpeded optical access from above and below the container.

3.4.2 Computer control

With the vertical control system, an important design criterion was digital computer control. As shown in Figure 3.5, each stepper motor is driven by a ViX controller which in turn is controlled by one computer. The controllers come with a software interface called Easi-V which provides a complete programming language with a number of present motion profiles as well as the ability to define an arbitrary motion profile. One software program can be called upon to drive multiple actuators individually. Given the symmetry of the setup, the two motors follow the same commands and the result is mirror symmetrical motion.

During construction and testing, constant speed motion was chosen for the motion profile; the moving wall velocity was ± 1 mm/s with ramp-up acceleration of ± 3 mm/s. The actuator system is capable of increasing or decreasing the velocity and acceleration values by an order of magnitude.

3.5 Optics

Capturing the motion of the fluid interface presented the biggest challenge. The design goal was to capture the dynamics of the water-air interface, $z = h(x, y, t)$, with a sampling frequency at the drive frequency. The target sample rate was 20 Hz which meant that waves oscillating at 10 Hz were sampled twice a period, up and down. The Fourier transform profilometry (FTP) technique was chosen due to its demonstrated success in measuring gravity waves in a fluid dynamics experiment [16]. While a transmission-mode technique with similar capabilities exists [17], it is difficult to implement without affecting the surface tension of water.

3.5.1 Fourier transform profilometry

The FTP setup consists of a camera recording images, a projected grating pattern and an object whose height is to be measured. The output of the technique is a height measurement for each pixel in a camera image.

The general crossed optical-axes geometry is displayed in Figure 3.7. A camera and projector are both a distance L from the reference plane O and separated by a distance D. In the limiting case where the optical axes are aligned, $\theta = 0$, both the geometry and mathematical formulas are simplified. A fringe pattern with

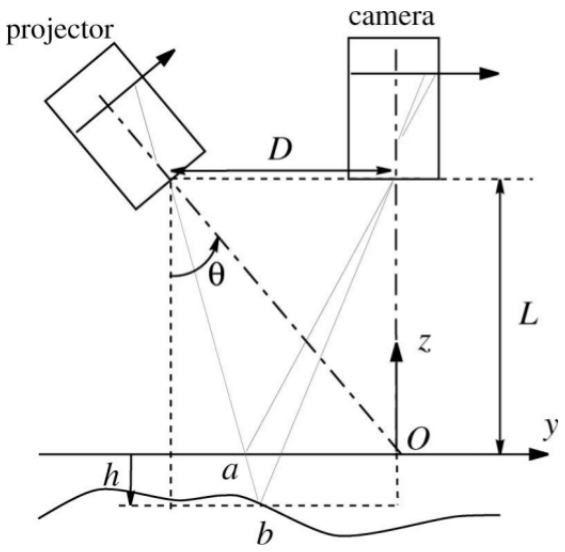

Figure 3.7: The setup [18] consists of a projector which displays a fringe pattern onto a deformed surface b, relative to the reference plane a, which is captured by the camera separated by a distance D. The deformed surface results in a deformed fringe pattern with phase offsets $\Delta\psi(y)$.

the fringes varying in the y-direction is projected onto a general object with a surface topography of interest. A camera records an image of the fringes on the object from which the height is determined, $z = h(x, y)$. Here and elsewhere, x and y are coordinates in the images recorded by the camera. Measurement of the deformation of the fringes, relative to the fringes on a reference plane, is a phase $\Delta\psi$ from which the height of the object, here a fluid interface, is computed.

The phase-to-height relation is arrived at through geometric arguments introduced by [19] and later corrected [18],

$$h(x', y') = \frac{L\Delta\psi}{\Delta\psi - \omega_0 D} \tag{3.3}$$

where $x' = x - \frac{h}{L}x$ and $y' = y - \frac{h}{L}y$ are the corrected image coordinates. The fringe frequency ω_0 is the frequency of the recorded fringe pattern in radians/length.

Measuring the phase shift $\Delta\psi$ is analogous to measuring the height. Since the fringes have a well-defined frequency by design, taking a Fourier transform of the images yields a power spectrum which is peaked at the fringe frequency ω_0. The phase shift is determined by filtering around this peak frequency [19].

3.5.2 Implementation

The camera is positioned directly above the projector on a vertical stage; see Figures 3.3 and A.11. The distance between the optical axes of the camera and projector is fixed at 11.4 cm (4.5 in) since they move together on the vertical stage. To view the fluid interface from above, a mirror is positioned horizontally across from the camera on another vertical stage with the container positioned below the mirror. The optical path length is reduced by lowering the projector and mirror using the vertical stages. The field of view may be reduced in the camera by optically zooming in, and the projector's resolution (the size of the projected pixel) may be adjusted similarly.

The surface conditions of the fluid interface are a key consideration. When imaging an opaque and diffuse material, incoming light is scattered in all directions and the camera captures light from the entire surface. However with a reflective

surface like water, incoming light rays reflect back at a unique angle so an image of surface waves captures only the surfaces angled such that light from the projector is reflected into the camera. This reflection-mode imaging technique is often used to image Faraday waves and produces excellent images for qualitative study; see Figure 3.8.

For the FTP technique to work the surface must be opaque and diffusive. For water to be used as a working fluid, a white pigment is added. Fortunately, titanium dioxide, which we use, was well-characterized [20] and does not affect the properties of water. Most importantly, the pigment is provided as a chemically pure powder without surfactants or other chemicals which can add a surface film and affect the surface tension of our water, both of which must be avoided in a controlled experiment.

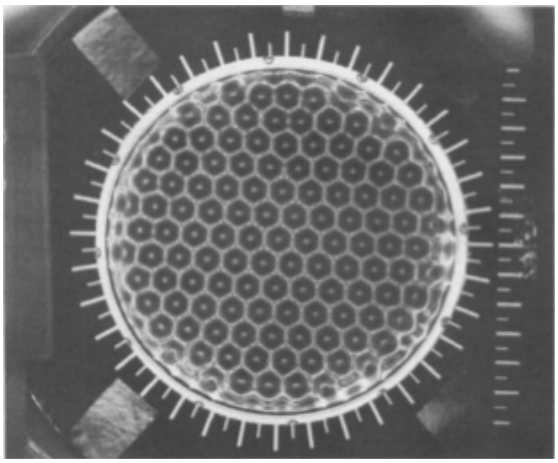

Figure 3.8: The Faraday pattern [6] is visualized using circular lighting such that the camera records reflected light when the surface normal is between 2.4° and 3.1° from horizontal.

Chapter 4

Optical measurement demonstration

The results shown below in a series of figures demonstrate the imaging and measurement capability developed for the study of time-dependent Faraday wave patterns. A number of challenges were overcome by optimizing parameters in the optics setup and post-processing using extensive trial and error. We demonstrate 3D megapixel surface height sampling with millimeter height resolution and a sample rate of 20 Hz.

One challenge was capturing sufficient information in images to be useful for later processing. Initially, images used less than 1% of the dynamic range of the camera which resulted in a poor signal-to-noise ratio and an unreliable height calculation. This challenge was addressed in part by optimizing the brightness and contrast of the projected grating image in Figure 4.1 to utilize the full dynamic range of the projector, from white to black. Additionally, the geometry of the

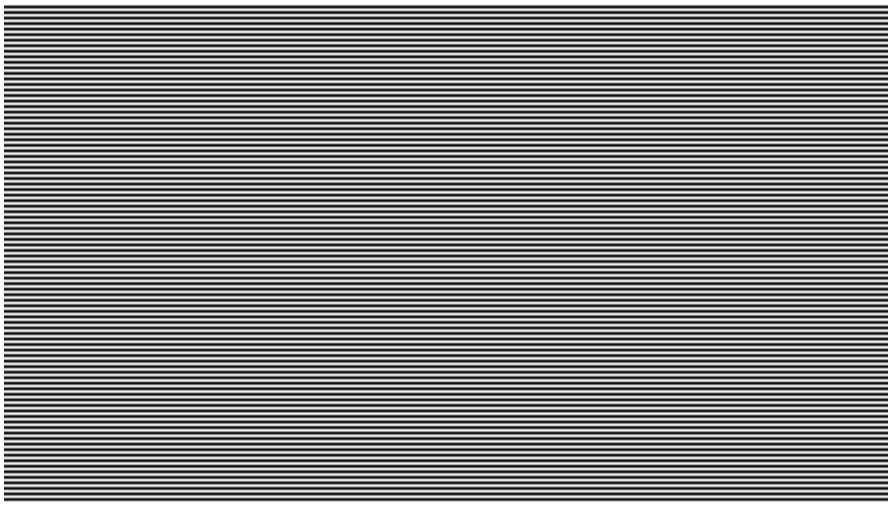

Figure 4.1: Digital image with the sinusoidal fringe pattern with 90 fringes. The resolution is 1920 x 1080 (1080p HD).

camera/projector system was optimized while maintaining a field of view of 15 cm x 15 cm. The contrast of the imaged fringes in Figure 4.3 was improved to 10%.

Compounding the imaging challenge is the direct reflection of light from the projector into the camera. An example of these reflections is the bright spots at the bottom of Figure 4.4. These reflections saturate the pixels and the information in these pixels is lost. Direct reflections were minimized by choosing the offset between the projector and camera so incoming rays were reflected out of the field of the camera. Such reflections completely avoided only in the quiescent reference image in Figure 4.3. Since the bright spots in Figure 4.4 are confined to the

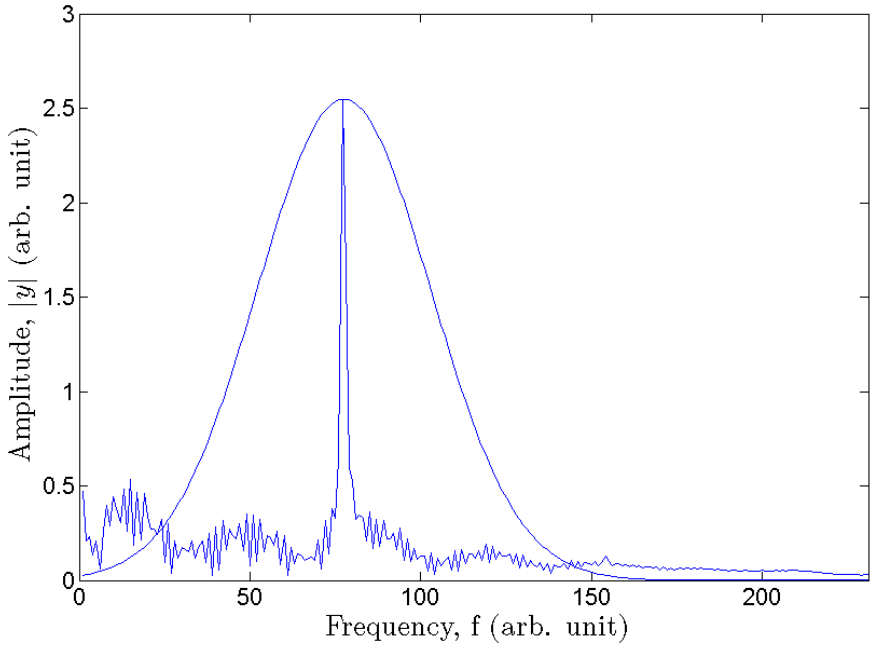

Figure 4.2: The amplitude of the Fourier spectra is plotted along with the Gaussian filter centered on the maximum(the Gaussian filter is not plotted to scale). The axes units are based image pixels but are arbitrary. The peak amplitude is located at the fringe frequency, here 77, and the width of the filter is scaled to one third this value, $\sigma = 25$. The zero frequency content was filtered prior to this step.

bottom of the image, the effect is a reduction in measured area rather than an altogether unusable measurement.

The outlines of the analysis routine are well documented [21, 19, 18], but present the data analysis without necessary addressing the subtle difficulties. The key step, shown in Figure 4.2, is the filtering of the Fourier spectra about the fringe frequency. The width of the Gaussian filter required fine-tuning on a case-by-case basis for best results. In general, the width of the window is one third

the fringe frequency which ensures the window is broad enough to capture the phase information of the peak harmonic while filtering unwanted noise from other carrier harmonics.

To further aid the visibility of the fringes, the diffusivity of our transparent working fluid, water, was enhanced with the addition of is the white pigment titanium dioxide. However, the pigment is not water soluble and experimentation found that mechanical stirring dispersed it into the water. Settling of the particles with time is a concern but was shown to be mitigated by the mixing effect of gravity-capillary waves generated a horizontal wavemaker [20]. Whether Faraday waves generate sufficient mixing to prevent settling is an open question; in any case, the effect of settling on the measurement of the fluid interface can be measured and accounted for.

The results shown below are a sample of the analysis. Each video frame is processed from which the surface height is extracted. The result is a video or animation where each frame looks like Figure 4.4. Further data analysis such as automated pattern modeling and pattern identification is possible since the data are simply a series of 2D matrices.

Parameter	Value	Comments
Frame rate	20 frames/sec	Imaging frame rate
Bit depth	8 bits	8 bits per pixel
Captured frames	1000	50 seconds
Image resolution	1280 x 1024	Pixels, full resolution
Projector resolution	1920 x 1080	Pixels, full resolution
Driving frequency	20 Hz	Wave frequency is 10 Hz
Image contrast	0.10	Used 10% of the dynamic range of the camera
Pigment concentration	12.5 g/L	Titanium dioxide in pure water
Fluid depth	0.89 cm	Depth of water in container
D	11.4 cm	Distance from camera to projector
L	63.5 cm	Distance from camera to fluid

Table 4.1: The main design goals are driven by the vertical forcing, horizontal motion, and measurement capabilities.

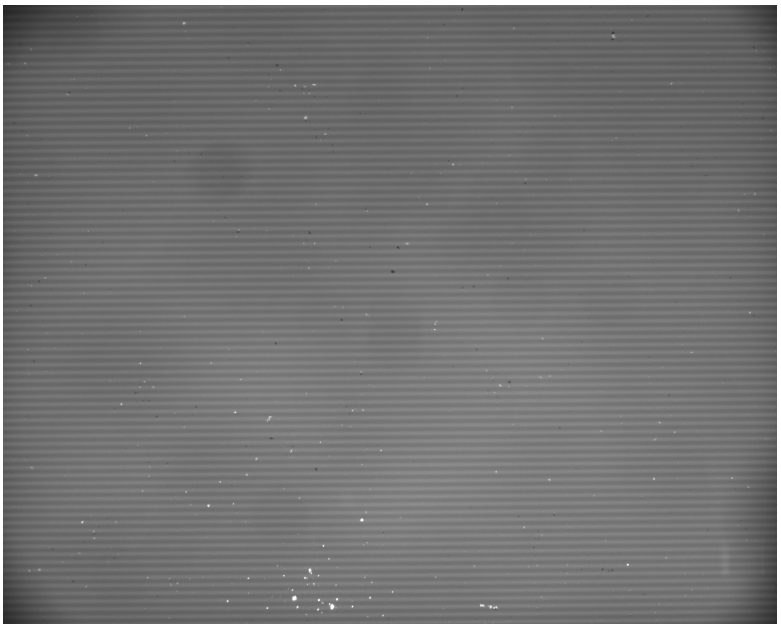

Figure 4.3: This is a unaltered image of the projected fringes on a flat surface of water and defines the reference plane for this image sequence.

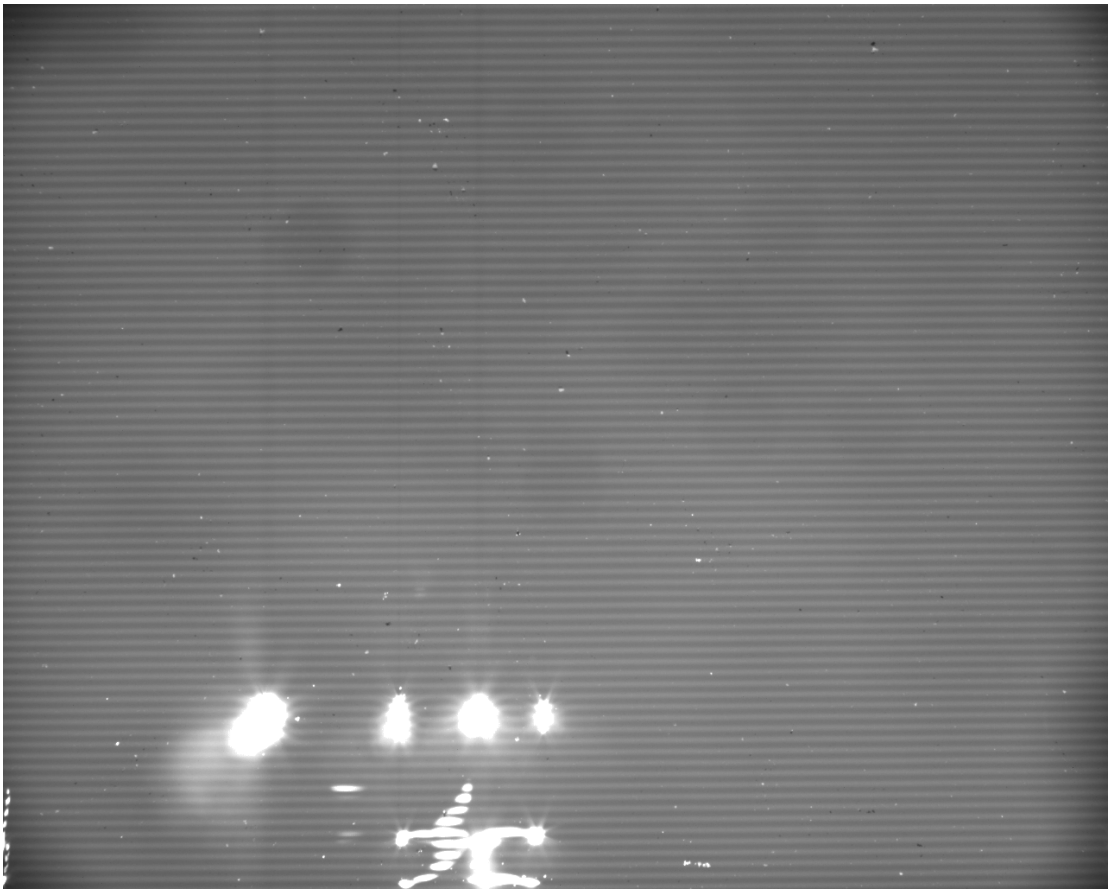

Figure 4.4: An image captured later after the formation of Faraday waves which are not visible. The bright spots at the bottom on the image is the projector filament since once standing waves form with a sufficiently large slope, light is reflected from the projector directly into the camera.

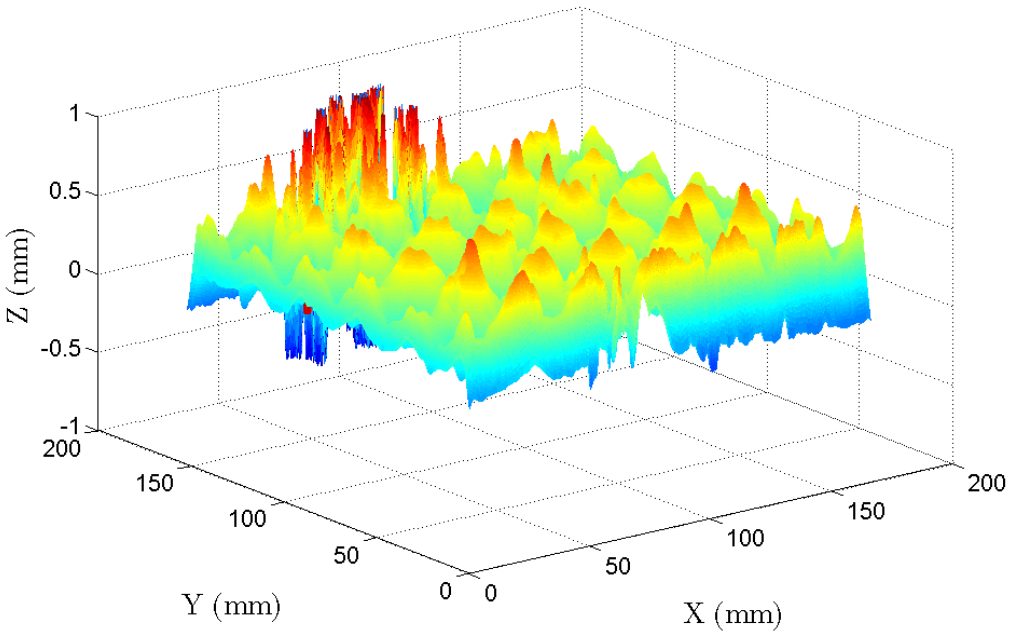

Figure 4.5: Extracted height from figure 4.4; note the z scale is 2 mm while the lateral scale is 200 mm. The spurious points around $Y = 200$ are located where the glare saturated the pixels.

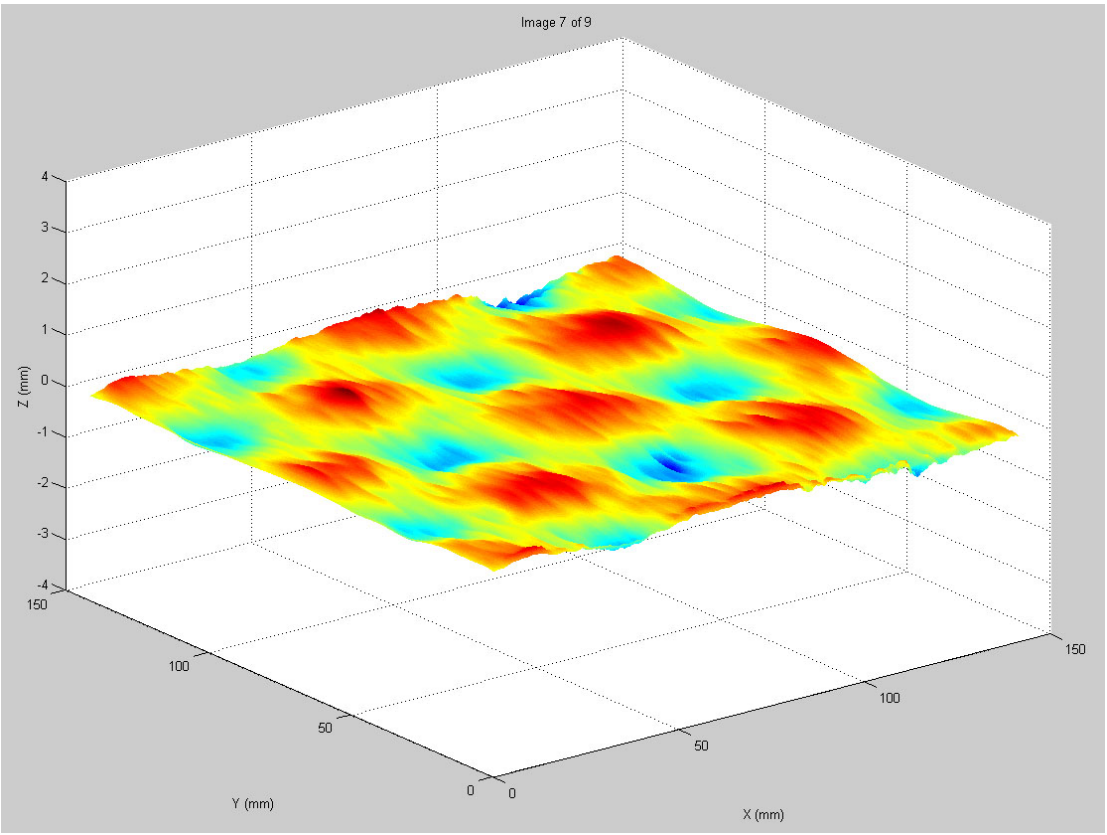

Figure 4.6: Here is second image from another experimental trial under different conditions which again demonstrates the measurement capability of the optics setup.

Chapter 5

Conclusion

Physical problems on time-dependent domains are common in nature; a theoretical treatment of such problems motivated this experiment on Faraday waves as a case study. For the study of Faraday waves on time-dependent domains, an experimental apparatus was built where Faraday waves form in a container of variable dimensions. To quantitatively capture the Faraday wave patterns, an optical measurement system capable of resolving the patterns in space and time was implemented.

Faraday waves are generated by vibrating a container of fluid vertically using a vibration system composed of a linear amplifier, shaker, and signal generator. The necessity to place the horizontal motion system on top of the vertical shaker led to a number of challenges, namely that the system must remain balanced, tolerate vertical vibration, and be light. In response to these challenges, two bespoke lin-

ear actuators incorporating small stepper motors, which move the symmetrically opposing walls, were constructed .

The study of Faraday waves, particularly on time-varying domains, called for a measurement method capable of recording the motion of a fluid interface in space and time, $z = h(x, y, t)$. The FTP technique provides a single-shot method which is scalable in sample rate (as quickly as images can be captured) as well as in resolution (depending on the resolution of the camera and projector). We demonstrated a fluid interface measurement using a megapixel image captured at 20 Hz with an anticipated resolution of 1 mm in height across a relatively large, 10 cm x 10 cm, area.

Although the FTP technique is a powerful tool, its implementation for use in fluid interface measurements was not straightforward. The surface of water is reflective and transparent and thus the opposite of the diffuse and opaque surface for which the technique was developed. By adjusting the optical geometry (camera/projector separation and optical path length) and the titanium pigment concentration, a solution was found which mitigated reflections while projecting a bright fringe pattern.

Future work on the experiment will require a detailed calibration of horizontal actuators, vertical vibration, and optical profilometry. To date, only cursory calibrations have been performed, principally for troubleshooting purposes. The

vertical and horizontal actuators should present no difficulty to calibrate, when operating individually as well as operating simultaneously. A key question to be addressed prior to running controlled experiments is the quantification of noise or undesirable acceleration to which the fluid is exposed.

An improvement that can be made is in the integration of the different functions of the experiment. The current setup operates the horizontal and vertical motion as wells as and measurement system independently even though the capability of simultaneous, unified control exists. It would be advantageous for all the components to have a common interface, so that for example, the acceleration reading can be associated with each fluid interface measurement.

The constructed setup will help one to understand Faraday waves on time-dependent domains, the knowledge of which will be useful in a wider class of systems which was the motivation for the present work.

Bibliography

[1] M. Faraday. On the forms and states assumed by fluids in contact with vibrating elastic surfaces. *Philos. Trans. R. Soc. London*, 52:319–340, 1831.

[2] T.B. Benjamin and F. Ursell. The stability of the plane free surface of a liquid in vertical periodic motion. *Philos. Trans. R. Soc. London*, 225:505–515, 1954.

[3] M.T. Westra, D.J. Binks, and W. van de Water. Patterns of Faraday waves. *J. Fluid Mech.*, 496:1–32, 2003.

[4] P. Chen and J. Viñals. Amplitude equation and pattern selection in Faraday waves. *Phys. Rev. E*, 60:559–570, 1999.

[5] S. Ciliberto and J.P. Gollub. Chaotic mode competition in parametrically forced surface waves. *J. Fluid Mech.*, 158:381–398, 1985.

[6] W.S. Edwards and S. Fauve. Patterns and quasi-patterns in the Faraday experiment. *J. Fluid Mech.*, 278:123–148, 1994.

[7] H. Arbell and J. Fineberg. Pattern formation in two-frequency forced parametric waves. *Phys. Rev. E*, 65, 2002.

[8] E. Knobloch and R. Krechetnikov. Stability on time-dependent domains. *J. Nonlinear Sci.*, 24:493–523, 2014.

[9] S. Douady. Experimental study of the Faraday instability. *J. Fluid Mech.*, 221:383–409, 1990.

[10] F. Simonelli and J. Gollub. Surface wave mode interactions: effects of symmetry and degeneracy. *J. Fluid Mech.*, 199:471–494, 1989.

[11] J. Bechhoefer, V. Ego, S. Manneville, and B. Johnson. An experimental study of the onset of parametrically pumped surface waves in viscous fluids. *J. Fluid Mech.*, 288:351–381, 1995.

[12] S. Douady and S. Fauve. Pattern selection in Faraday instability. *Europhys. Lett.*, 6:221, 1988.

[13] O. Lioubashevski, H. Arbell, and J. Fineberg. Dissipative solitary states in driven surface waves. *Phys. Rev. Lett.*, 76:3959–3962, 1996.

[14] D. Binks and W. van de Water. Nonlinear pattern formation of Faraday waves. *Phys. Rev. Lett.*, 78:4043–4046, 1997.

[15] M. Shats, H. Xia, and H. Punzmann. Parametrically excited water surface ripples as ensembles of oscillons. *Phys. Rev. Lett.*, 108, 2012.

[16] P.J. Cobelli, V. Pagneux, A. Maurel, and P. Petitjeans. Experimental study on water-wave trapped modes. *J. Fluid Mech.*, 666:445–476, 2011.

[17] W.B. Wright, R. Budakian, and S.J. Putterman. Diffusing light photography of fully developed isotropic ripple turbulence. *Phys. Rev. Lett.*, 76:4528–4531, 1996.

[18] A. Maurel, P.J. Cobelli, V. Pagneus, and P. Petitjeans. Experimental and theoretical inspection of the phase-to-height relation in Fourier transform profilometry. *J. Opt. Soc. Am.*, 48:380–392, 2009.

[19] M. Takeda and K. Mutohi. Fourier transform profilometry for the automatic measurement of 3-D object shapes. *Appl. Opt.*, 22:3977–3982, 1983.

[20] A. Przadka, B. Cabane, V. Pagneux, A. Maurel, and P. Petitjeans. Fourier transform profilometry for water waves: how to achieve clean water attenuation with diffusive reflection at the water interface? *Exp. Fluids*, 52:519–527, 2012.

[21] M. Takeda, H. Ina, and S. Kobayasi. Fourier-transform method of fringe-pattern analysis for computer-based topography and interferometry. *J. Opt. Soc. Am.*, 72:156–160, 1982.

Appendix A

Operating manual

This appendix is a basic operating manual for the experiment. Each experimental function is presented at an operational level starting with §A.1 on vertical motion, §A.2 on horizontal motion, and §A.3 on the optics setup and implementation.

A.1 Vertical motion

This section contains guidelines, procedures and safety information on the vertical motion system consisting of the Labworks vibration system, LabVIEW computer interface, and accelerometers.

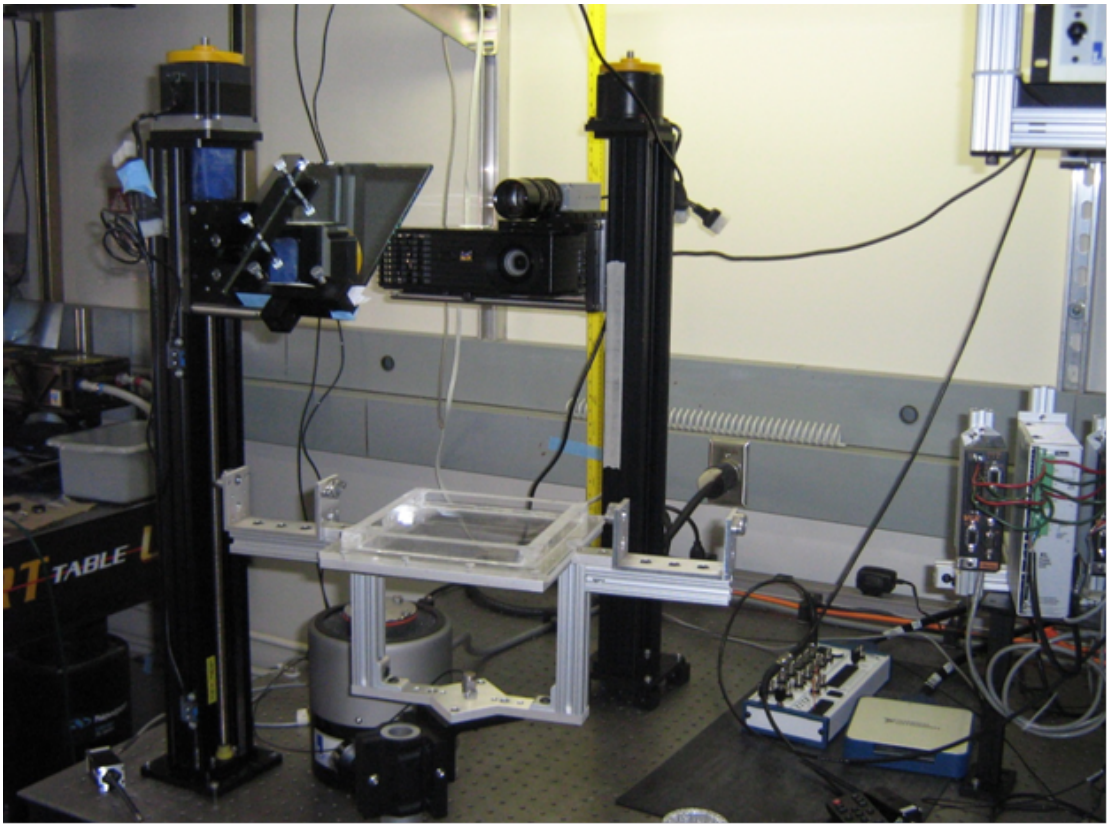

Figure A.1: Partially disassembled experimental setup with the apparatus removed from the shaker and fastened to an optical post to prevent damage to the shaker while work is done on the experiment. The stepper motors and sliding wall assemblies have also been removed.

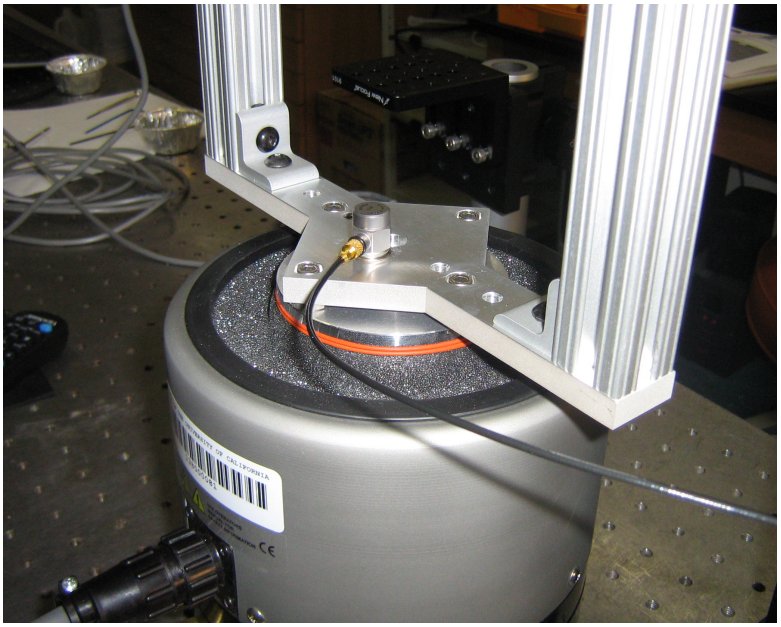

Figure A.2: Pictured is the shaker and its connection to the linear amplifier (lower left corner) and the accelerometer (center) mounted to the base plate.

A.1.1 Shaker

The Faraday apparatus is mounted to the shaker mounting plate with five 10-32 socket head cap screws which meet the length specification in the Labworks manual. General precautions:

1. Do not twist the armature. Any work on the apparatus (eg fastening screws) should be done off the shaker.
2. Keep metal filings or any other ferromagnetic materials away from the shaker.
3. Keep the area around the shaker dry.
4. The shaker has mechanical stops enforcing 1 inch of vertical displacement. Generating large acceleration at low frequencies can break the stops and damage the shaker.

Figure A.3: Front panel of the amplifier with a voltage and current indicator, on/off power switch, and gain knob.

5. At audible frequencies the shaker and amplifier are a powerful sound system; use ear protection for large amplitude motion at frequencies above 50 Hz.

6. Running the system at the top of the amplifier's output range requires the cooling blower prevent the shaker from overheating.

A.1.2 Linear power amplifier

The amplifier takes the signal provided by the LabVIEW DAQ and amplifies it to drive the shaker. The amplifier is run in `VOLTAGE MODE`. The gain knob, when not in use, is turned completely counterclockwise to the `RESET` position.

1. Check the cooling vacuum pump for obstructions before Step 2.
   (a) Check that the Faraday apparatus is securely fastened and balanced.
   (b) The GAIN knob should be in the `RESET`, or off, position as shown.
2. Turn on the amplifier. The vacuum pump will start if it is plugged into the back panel of the amplifier.

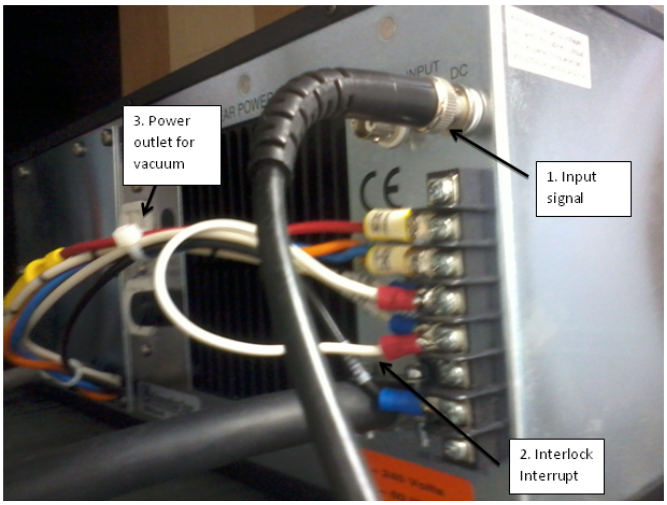

Figure A.4: Back panel of the amplifier with labels of the input signal, interlock interrupt and the power outlet.

3. Provide a low-level signal to amplifier ($\sim$ 100 mV pk-pk)
4. Slowly increase the gain, turning the gain knob clockwise, rotating 45° or less from the off position is typical.
5. With the range set by the gain on the amplifier, further adjustment is made using the DAQ/LabVIEW VI
6. Turn DAQ output to 0 V and turn gain down to `RESET` (off position)
7. Allow amplifier to cool for a few minutes before powering off

Three connections are made on the back panel by the user: (1) the input signal from the DAQ, (2) the interlock interrupt, and the (3) power to the cooling blower. The amplifier has a safety mechanism requiring the cooling blower to be installed if the interlock is not shorted as shown. More information is available in the amplifier manual provided by Labworks.

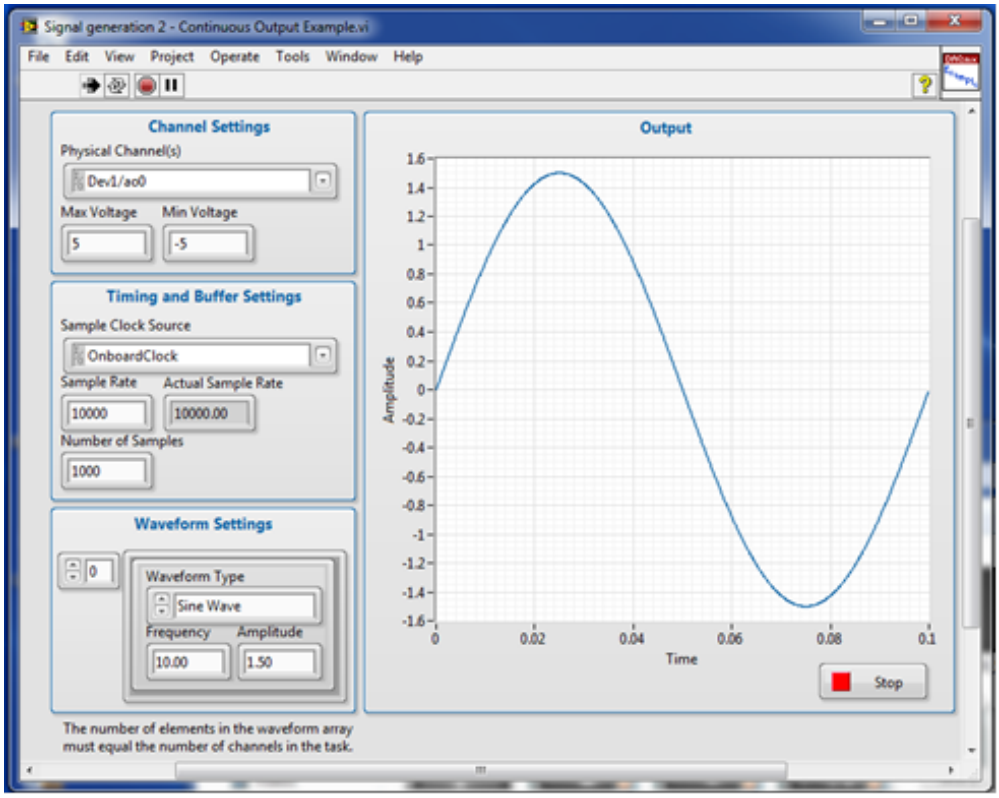

Figure A.5: `Signal generation 2 - Continuous Output Example.vi` is a simple sine wave generator provided by LabVIEW with real-time control of the frequency and amplitude. The output shown is a 3 V peak-to-peak 10 Hz sine wave sampled at 10,000 samples/second with one period stored in the buffer memory.

A.1.3 Signal generation in LabVIEW

The BNC analog output 1 (`AO1`) is connected to the input on the back panel of the amplifier. Figure A.5 shows VI which generates a signal, displays it on the screen, and outputs it through the DAQ device. Before running the program set the Max Voltage and Min Voltage (±5 V), the Sample Rate and the Number of Samples. The signal discretized in time by the sample rate and by the number

Figure A.6: Two accelerometer signal conditioners with only the top in use. The BNC output is split and sent to the DAQ and oscilloscope.

of samples determines the length of the signal stored in the buffer memory — the signal is repeatedly read out from the buffer to the DAQ. The frequency and amplitude can be adjusted while the program is running. It is a good practice to start and stop the VI from a zero amplitude signal.

A.1.4 Acceleration measurement

Acceleration is measured using two Brüel & Kjær accelerometers. They are constant current line drive (CCLD) type sensors powered by the signal conditioner. The green LED light on the signal conditioner indicates that it is receiving power

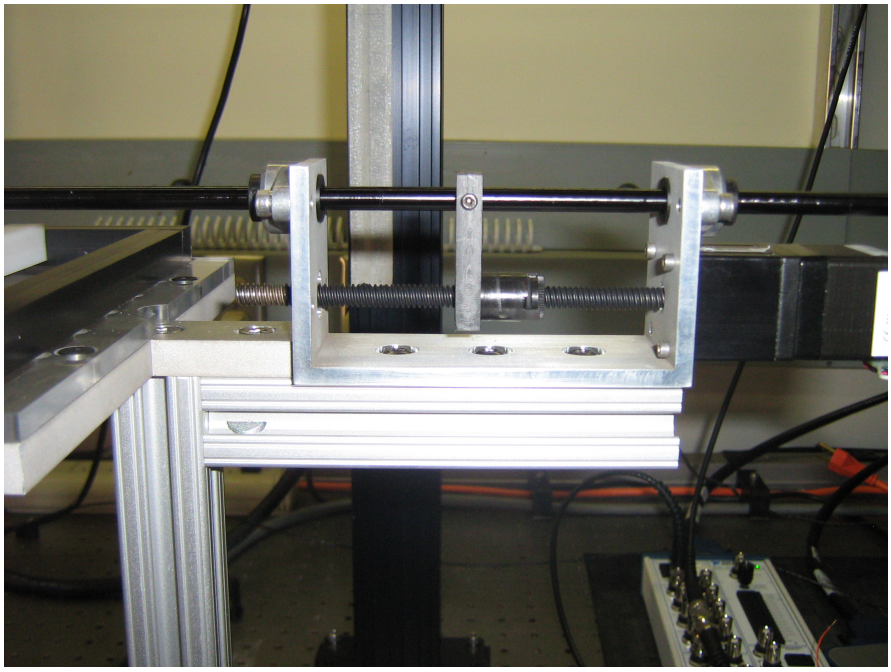

Figure A.7: The linear actuator is driven by a stepper motor, the traveling nut connects to the shaft which is connected to the moving wall.

from the AC adapter. To enable measurement from the accelerometer, push the `CCLD` and `POWER` toggles to `ON` from the signal conditioner front panel.

The sensors both are rated at 10 mV/g so when gain is set at `x100` the output voltage is 1 V/g. The sensors have a range of ±50 g and typical motion produces low-level signals requiring amplification; the gain can be reduced should the signal exceed 10V. The documentation with each sensor gives the factory-provided calibration 10.10 mV/g and 10.44 mV/g.

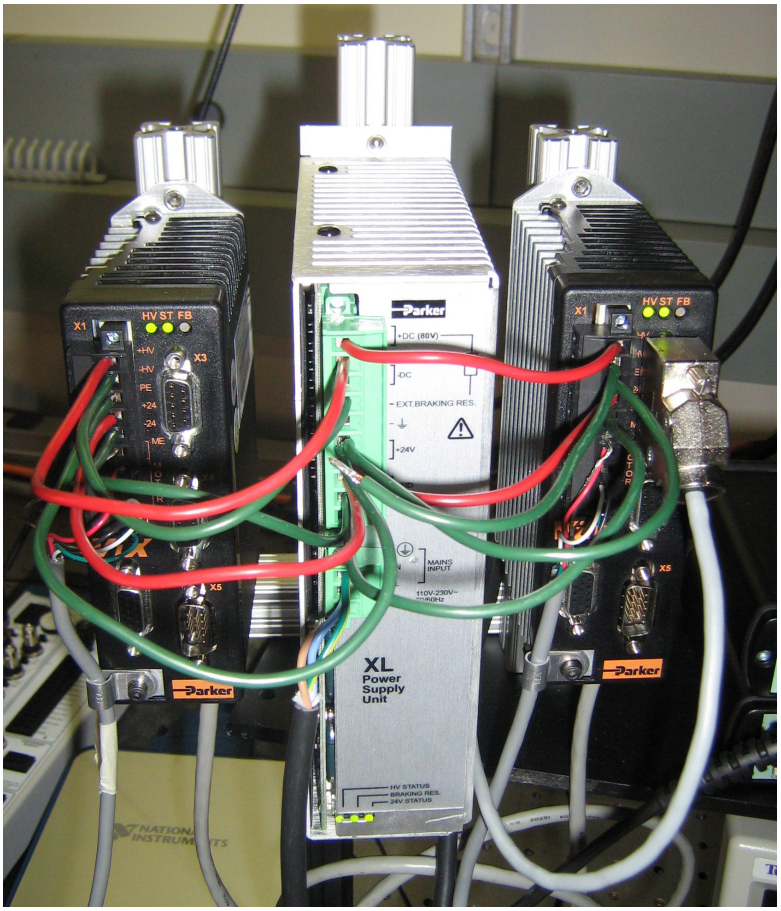

Figure A.8: Driving the two stepper motors are three pieces of Parker electronics: in the center is a power supply which powers the controllers on the left and right.

A.2 Horizontal motion

The horizontal actuator system is shown schematically in figure 3.5. Each controller is responsible for driving a single stepper motor which moves one wall. Control of the stepper motors is open-loop, no position feedback is available. Both controllers are powered by a single power supply.

In Figure A.8 we see the equipment that runs the two linear actuators. In the center is the power supply, on the right is Controller 1 and on the left is Controller 2. The three pieces of equipment are fastened to a simple structure designed to keep the equipment compact and accessible.

The biggest safety hazard to be aware of is the 110 V wall-power connection to the power supply; these connections should be tight and with no exposed wire.

A.2.1 Controller connections

The RS232 connection with the computer is made using the Parker-supplied RS232 cable and a USB-to-RS232 adapter. The connection will not work without the Parker RS232 cable because Parker use a non-standard pin configuration.

A CAT5 ethernet cable (also called RJ45) daisy-chains the two controllers. The bottom front connection (OUT) on the right controller is made with the bottom rear connection (IN) on controller on the left (see page 42 in VIX manual).

Both controllers are powered by the same power supply. The top half of the controller connections are made with the power supply and the bottom half are motor connections. The power supply's connection pins are duplicated in pairs so wires in Figure A.8 alternate going to the left controller and right controller.

The cable hard-wired to the stepper motor terminates in 5 separate strands which constitute the motor connections. Making the connections requires identi-

X1 Pin Number	Function	Wire Color	Class
10	+ High Voltage	Red	
9	- High Voltage	Green	
8	Protective Earth	Green	Power Connections
7	24V DC	Red	
6	24V Ground	Green	
5	Motor Ground	Bare wire	
4	Motor Phase (A+)	Red	
3	Motor Phase (A-)	Black	Motor Connections
2	Motor Phase (B+)	White	
1	Motor Phase (B-)	Green	

Table A.1: Pin connections on the front panel of each controller. Half go to the power supply and half to the stepper motor.

fying which wire goes into which pin: motor cables are identified using the Parker Quick Start Guide, and pins in the controller are identified in the ViX Connector Pin Layout (ViX manual page 27).

Table A.1 lists the wiring of the controller: power connection in and motor connections out. The X1 connection block is the top left and pin numbering convention is the bottom pin is 1 and the top pin is 10.

The `M11xx Option` values in Figure A.9 provide the NEMA 11 stepper motor parameters and are used during the Easi-V setup below.

A.2.2 Actuators control

The two linear actuators are controlled using the EASI-V software.

1. Launch the Windows XP-Mode virtual machine

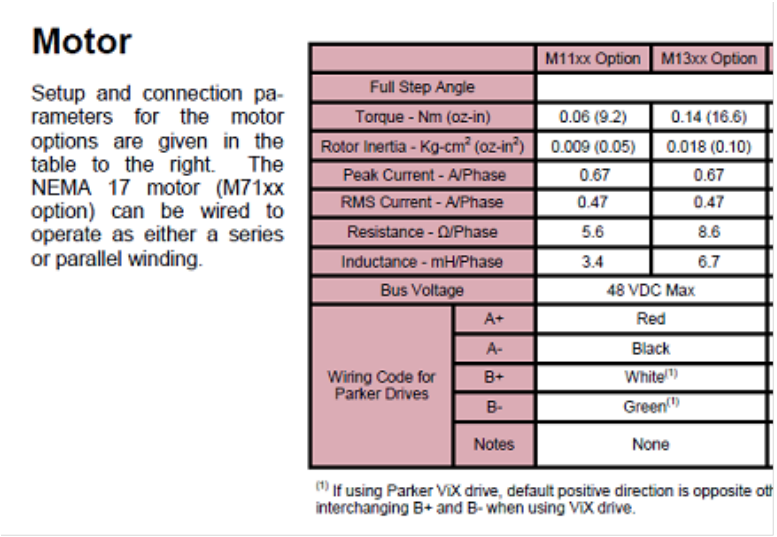

Motor

Setup and connection parameters for the motor options are given in the table to the right. The NEMA 17 motor (M71xx option) can be wired to operate as either a series or parallel winding.

		M11xx Option	M13xx Option
Full Step Angle			
Torque - Nm (oz-in)		0.06 (9.2)	0.14 (16.6)
Rotor Inertia - Kg-cm^2 (oz-in^2)		0.009 (0.05)	0.018 (0.10)
Peak Current - A/Phase		0.67	0.67
RMS Current - A/Phase		0.47	0.47
Resistance - Ω/Phase		5.6	8.6
Inductance - mH/Phase		3.4	6.7
Bus Voltage		48 VDC Max	
Wiring Code for Parker Drives	A+	Red	
	A-	Black	
	B+	White[1]	
	B-	Green[1]	
	Notes	None	

[1] If using Parker ViX drive, default positive direction is opposite oth
interchanging B+ and B- when using ViX drive.

Figure A.9: The technical details of the motor are provided in the `M11xx Option` column.

2. The RS232-USB connection isn't automatically detected. In the USB menu, attach the `USB-Serial Controller`. (The driver for the installed RS232 connection is in the .zip file on the DAQ Dell desktop.)
3. The controller should be powered on before attempting to connect
4. Launch Easi-V
5. Accept the default setting (Parker 250IM controller)
6. Click Connect
7. If successfully connected a DOS-style text interface is established with the controller
8. Start the program in the controller memory by typing `0GOTO(START)`

A.2.3 Motion profile

The code used to run the linear actuators is in Appendix C.1. Two lines of code set the speed, acceleration, distance and number of repetitions. The motion

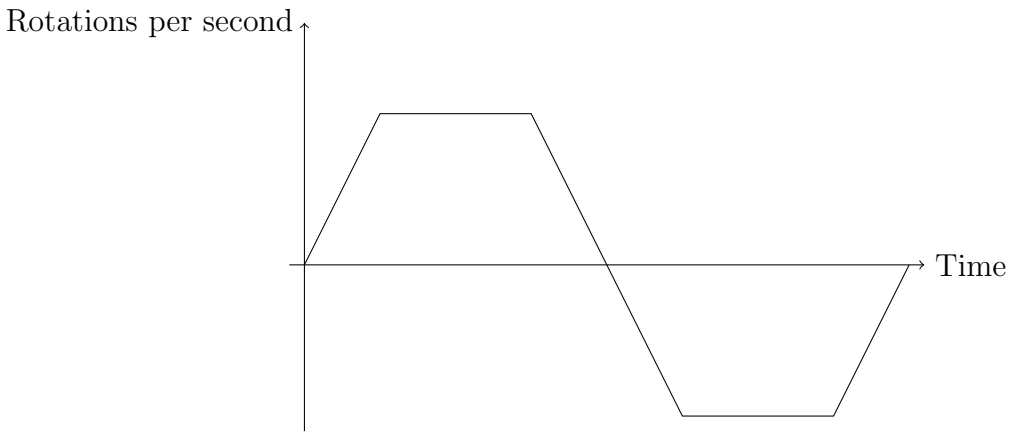

Figure A.10: Plotted is the motion profile control signal implemented by the ViX controllers and sent to both stepper motors.

profile in Figure A.10 is composed of 4 motion segments, repeated once: (1) constant acceleration (rps/s), (2) constant motion (rps) (3) constant deceleration, (4) change direction

Segments 1–3 are defined in line 25 which sets the parameters of the motion profile: `OPROFILE1(1,2,250000,.33)`

$1 = 1$ rps^2, the rate of acceleration

$2 = 2$ rps^2, the rate of deceleration

$250000 = 250,000$ steps, the total distance to travel

$.33 = 0.33$ rps, the rotation rate

The direction is changed in line 62 with the command `OH`.

The rotating leadscrew moves the traveling nut by 3 mm per rotation:

$$0.33 \text{ rotations/sec} * 3 \text{ mm/rotation} = 1 \text{ mm/s}.$$

Line 52 defines the number of steps per revolution:

`OMOTOR(201,0.5,50000,1000,4,2.80,3.40).`

$$50000 = 50,000 \text{ steps/rotation}$$

Therefore, the distance traveled in each direction is

$$250,000 \text{ steps}/50,000 \text{ steps/rotation} * 3 \text{ mm/rotation} = 15 \text{ mm}.$$

Browsing the 200 page documentation provided with the ViX controller, it is apparent they are highly configurable. Synchronizing the horizontal motion with the vertical motion, if desired, can be achieved by setting a trigger to start the pre-defined horizontal motion. That way, both the vertical motion and horizontal motion would be controlled through the same software — the Virtual Instrument in LabVIEW.

A.3 Optics

The camera is mounted directly above the projector, see Figure A.11, and the distance between the camera and projector is fixed at 11.4 cm (4.5 in) and they

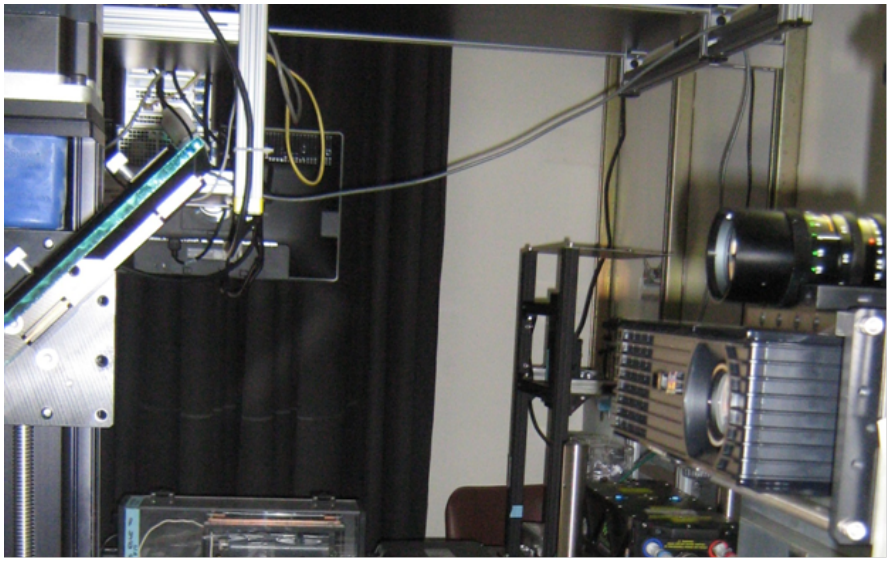

Figure A.11: Seen from the side, from left to right: are the vertical stage, mirror, plexiglass container, projector, and camera.

move together on the vertical stage. The mirror is positioned horizontally across from the camera with the container positioned below the mirror. The optical path length and field of view may be reduced by lowering the projector and mirror using the vertical stages. The field of view may be also be adjusted using the optical zoom on the projector and camera individually.

The ViewSonic Digital projector has a maximum resolution of 1080p (1920x1080) at 60 frames per second (fps). To limit flickering (brightness variation in the captured images) the projector may be operated at a reduced resolution but at its highest frame rate of 120 fps. Images captured at 30 fps average over many projected images and flickering is eliminated. The projector can alter the output digitally: adjusting the keystone (to correct for image distortion), reducing the

resolution, altering the brightness and contrast as well as via analog optics: zoom and focus.

The center of a projected image is above the optical axis of the projector; projected images are higher than the projector. Since the field of view of the camera and projected image need to overlap, the natural position of the projector is directly below the camera.

Figures A.11 and A.12 show the parallel optical axes configuration. Even though the projector is below the camera their fields of view overlap. The camera sits atop the projector and the vertical offset between the camera and projector is minimized because the range of measurable surface slopes increases as the camera and projector are brought closer together [19].

A.3.1 Projected grating images

Grating images are projected with the camera and projector stacked vertically such that the grating stripes are aligned horizontally.

The discrete representation of the cosine wave in Figure A.13 is apparent because larger grating frequencies, with fewer samples per sine wave, reduce measurement error [18]. The full resolution of figure A.13 is 1920 x 1080 pixels. It is stored as a 16 bit uncompressed png image. The sampling of the cosine function is chosen to maximize the dynamic range of the projected image. The grating in

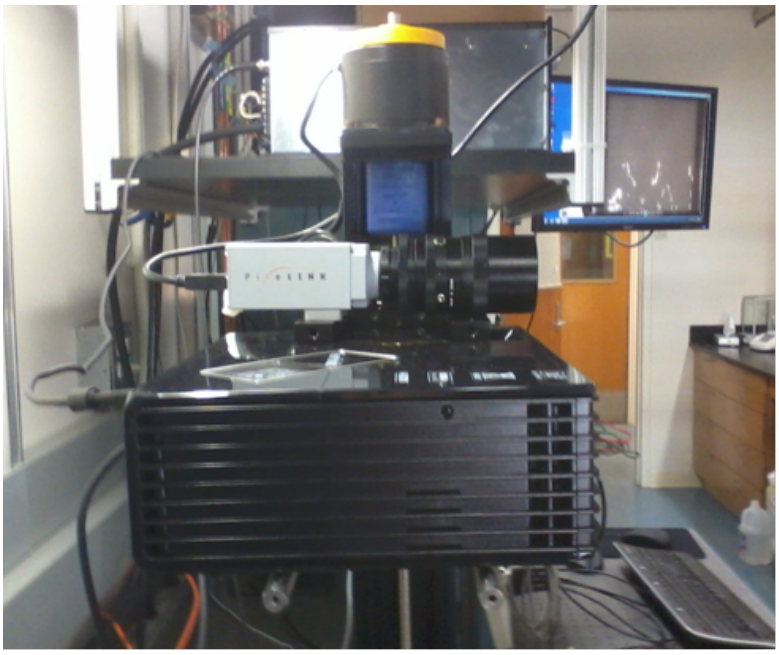

Figure A.12: Seen from the side is the projector and camera supported by a vertical stage.

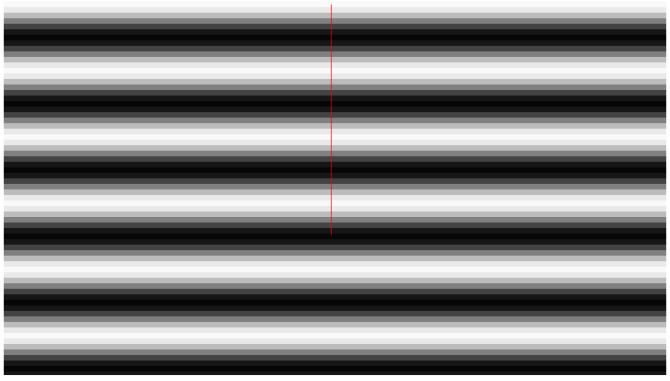

Figure A.13: A portion of a grating image, note the discrete steps in grayscale as the pattern varies between white and black. The grayscale values are plotted in figure A.14 along the line segment shown in the center of the image.

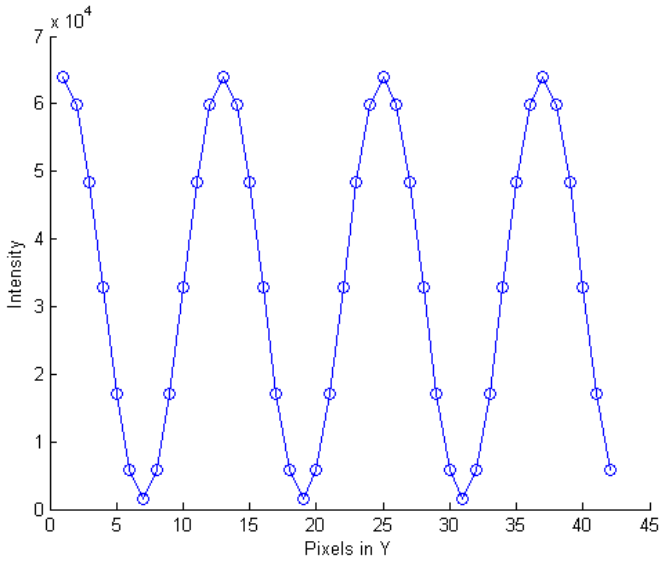

Figure A.14: Profile plot of the grayscale intensity along the vertical line in Figure A.13.

Figure A.13 is plotted along a vertical segment in Figure A.14, with 12 sampled grayscale points per cycle, the grating frequency is $1080/12 = 90$ and there are a total of 90 stripes.

$$I(y) \approx \cos\left(\frac{2\pi f_0}{N}x\right),\ x = 1, 2, 3, \ldots N-1 \tag{A.1}$$

A.3.2 Image analysis progam

The MATLAB program `im_analyze5_2.m` processes a stack of images and returns the surface height in three stages: initialization, analyzing reference image, processing image stack.

The program operates at a low-level and requires user input during the first two steps to process the data properly. When processing the images in the list, set a number of debug points throughout the program to pause and examine figures or to perform calculations. The program, often produces unreliable results so results must be saved manually, using the `save` function in MATLAB. The program outputs a small movie showing each plotted figure in sequence.

	Task	Program Variable
1	Set image directory location	`im_dir`
2	Specify images to be analyzed	`im_list`
2a	1st image is reference image	`im_list(1)`
2b	Choose no more than 30 images due to memory limitation	
3	Input geometrical data	
3a	Distance from camera to reference plane	`L_0`
3b	Distance from projector to camera	`D`
3c	Pixel Pitch – physical size of pixels in image	`pixel_pitch`

Table A.2: Initialization phase tasks and variables.

	Task	Program Variable
1	Set region of interest	`ROI`
2	Check contrast	
2a	Poor contrast can limit the FTP technique	
2b	Choose no more than 30 images due to memory limitation	
3	Check window	`gauss_filter_ratio`
3a	The window should be centered on the peak of the plot	`L_0`
3b	Window needs to cut off before next peak	`D`

Table A.3: Analyzing the reference image, tasks and variables

	Task	Program Variable
1	Process the rest of the images in the list	
2	Save height data	`im.h`

Table A.4: Processing the image stack, the final result is stored in the variable `im.h`.

Here are a few final considerations:

1. set a debug point and save the variables in memory: the variable `im.h` contains the final result,

2. check how noise in horizontal and vertical directions compare.

3. excessively noisy images lead to problems in the angle function and jumps of 2π.

A.3.3 Variables used in MATLAB program

The variable `im` uses an advanced type of variable in MATLAB called a structured array (struct). A struct, in contrast with an n-dimensional matrix, can accommodate different types of data. Here, `im` contains matrices, strings and images.

Once the data are processed, a matrix of height data — one data point per pixel — may be plotted using the `surf` or `mesh` functions each of which plot $z = h(x, y)$. The 3D plots in §4 utilized the `mesh` function.

Variable Name	Description	Typical value	Comments
`im_dir`	Image Directory	`Trial 32_8\`	Locates stack of images or video, to process. 1st image is the reference.
`im_list`	Image List	`[10:30]` or `All`	Images or frames to read
`plots_on`	Generate Plots	2	Generate diagnostic plots, generally leave on
`L_0`	Length (mm)	`812.8`	Distance from camera to reference plane
`D`	Length (mm)	`120.65`	Distance from camera to projector
`pixel_pitch`	Pixel Pitch (pixels/mm)		
ROI	Region of Interest	`[200,90,1050,990]` or `off`	Defines a rectangle: X Start (1st column), Y start (1st row), X End (last column), Y end (last row)
`rotate_on`	Rotate Image	`0 or 1`	Rotates image gratings aligned horizontally
`high_pass_wid`	High pass window size	`80`	Width of filter centered on 0 frequency
`gauss_filter_ratio`	Gaussian filter ratio	`1/3`	Ratio of standard deviation of filter to wavenumber
`im`	Image struct	`1x21 struct array with fields: image name phase h`	1xN struct array for N images
`im.name`	Image name	`trial_32_80009.tif`	Image file name
`im.image`	Image data	`im(1).image = <1024x1280>`	Image data, stored as a matrix
`im.fft`	Fourier transform	`1/3`	Intermediate stage
`im.phase`	Phase data	`1/3`	Phase data, penultimate step
`im.h`	Height data	`1/3`	Final result

Table A.5: Variables in the image analysis program with a field value and brief comments.

Appendix B

Technical documents

B.1 Design components

Manufacturer	Model	Name	Description
Brüel and Kjær	Type 4513	Accelerometer	Accelerometer sensor
Brüel and Kjær	Type 1704-A-001	Signal Conditioner	Signal Conditioner and amplifier for accelerometer
Dell	Precision T7600	Computer	Computer
Edmund Optics	#41–405	Mirror	Optically-flat mirror: 4-6 Wave, 169mm x 194mm
Fisher Scientific	S25818	Titanium dioxide	100g, 98% TiO_2, white powder pigment
Labworks	LW–139.141–75	Vibration system	75 lbs shaker system
Labworks	ET-139	Shaker	Electrodynamic shaker
Labworks	PA-138	Amplifier	Linear power amplifier
Labworks	CB-152-139	Cooling blower	Cooling vacuum pump
Mathworks	Matlab	Matlab	Data analysis
Microsoft	Windows Virtual PC	Windows XP Mode	Software for XP emulator for Windows 7
National Instruments	BNC 2120	Connector terminal	BNC connector terminal
National Instruments	PCIe–6363	DAQ	Data acquisition card

Manufacturer	Model	Name	Description
National Instruments	LabVIEW	Labview	Software for data input/output
Parker-Hannifin	ViX 250IM	Controller	Stepper motor controller
Parker-Hannifin	XL-PSU	Power supply	80V motor power supply
Parker-Hannifin	LD28	Controller	Stepper motor controller
Parker-Hannifin	Easi-V	Easi-V	XP Software for ViX controllers
PixeLINK	PL-B741U	Camera	1.3 Mp monochromatic camera
PixeLINK	Capture OEM	Camera interface	Software interface to camera
Vexta	PK296-03BA-A3	Linear Stage	Leadscrew vertical stage with stepping motor
ViewSonic	PJD7820HD	Projector	Small digital projector

Table B.1: All of the equipment used for the experiment is listed by manufacturer.

B.2 Engineering drawings

Drawing title	Quantity	Material
Base Plate	1	Aluminum
Container bottom	1	Acrylic (Plexiglass)
Container support rim	1	Power supply
Horizontal beam	2	1010 profile T-Slot from 80/20
Leadscrew adapter	2	Delrin
Moving Wall	2	Delrin
Parallel container wall	2	Delrin
Perpendicular container wall	2	Delrin
Wall connector	2	Delrin
Sliding wall	2	Teflon
U-Channel	2	Aluminum
Threaded standoff	2	Delrin
Vertical beam	2	1010 profile T-Slot from 80/20

Table B.2: A table of the engineering drawings in the section.

6X ø .201 THRU ALL
1/4-20 UNC THRU ALL
1.000
1.400
1.000
ø 2.800
2.000
2.959
4.453
5X ø .201 THRU ALL
ø .375 ↧ .190
.375
2X ø .266 THRU ALL
ø .438 ↧ .250
1.850
3.953
90.00°
PROPRIETARY AND CONFIDENTIAL
THE INFORMATION CONTAINED IN THIS DRAWING IS THE SOLE PROPERTY OF <INSERT COMPANY NAME HERE>. ANY REPRODUCTION IN PART OR AS A WHOLE WITHOUT THE WRITTEN PERMISSION OF <INSERT COMPANY NAME HERE> IS PROHIBITED.
UNLESS OTHERWISE SPECIFIED:
DIMENSIONS ARE IN INCHES
TOLERANCES:
FRACTIONAL ±
ANGULAR: MACH ± BEND ±
TWO PLACE DECIMAL ±
THREE PLACE DECIMAL ±
INTERPRET GEOMETRIC TOLERANCING PER:
MATERIAL
Alum
FINISH
DO NOT SCALE DRAWING
NAME
DATE
DRAWN
RHR
9/23
CHECKED
ENG APPR.
MFG APPR.
Q.A.
COMMENTS:
Dimensioned from center for symmetry
APPLICATION
USED ON
NEXT ASSY
KFPL
TITLE:
Base Plate
SIZE
A
DWG. NO.
REV
5
SCALE: 1:2
WEIGHT:
SHEET 1 OF 1
SolidWorks Educational Edition
For Instructional Use Only

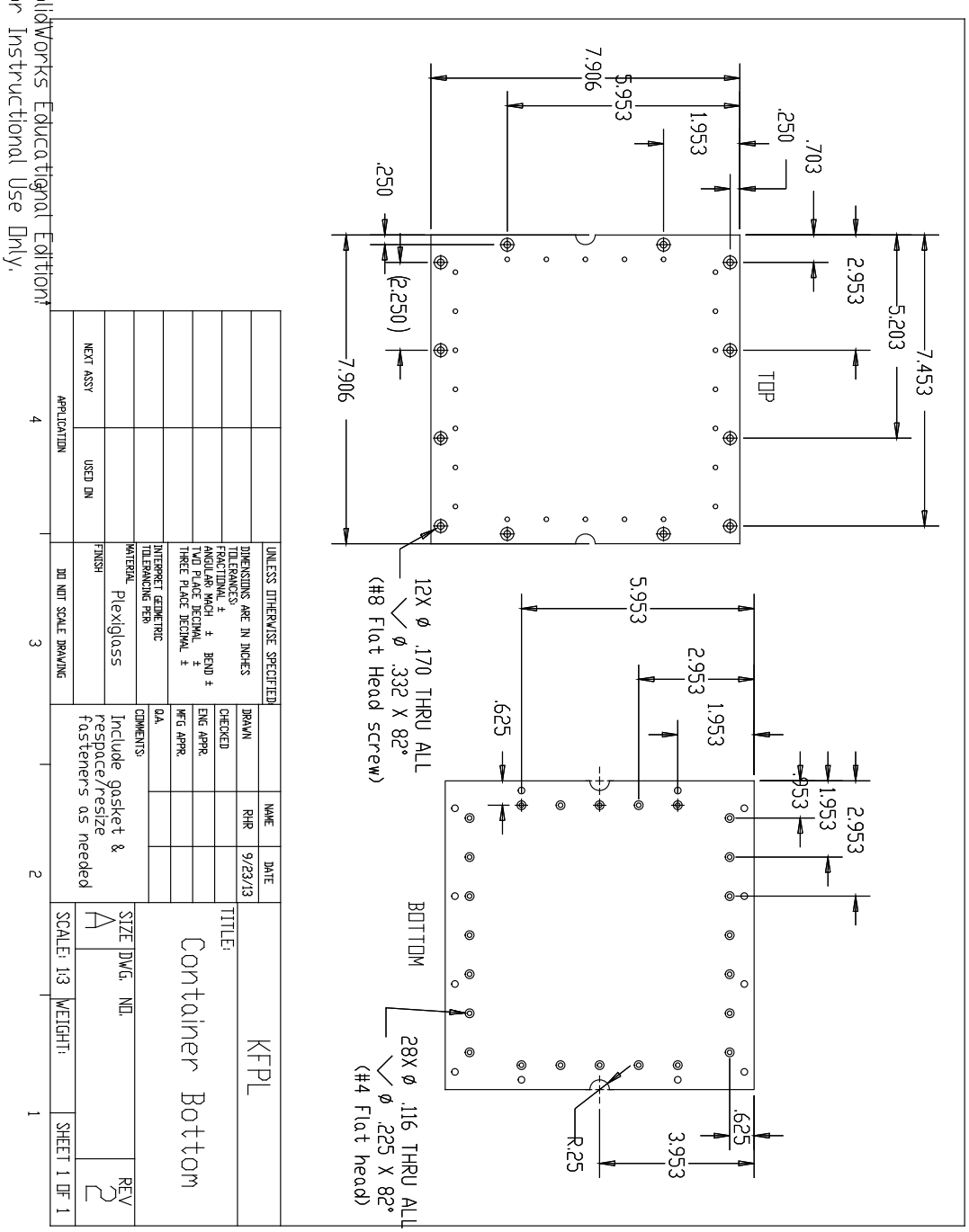
TOP
7.453
5.203
2.953
.703
.250
1.953
5.953
7.906
(2.250)
12X ø .170 THRU ALL
ø .332 X 82°
(#8 Flat Head screw)
BOTTOM
28X ø .116 THRU ALL
ø .225 X 82°
(#4 Flat head)
.625
3.953
R.25
UNLESS OTHERWISE SPECIFIED:
DIMENSIONS ARE IN INCHES
TOLERANCES:
FRACTIONAL ±
ANGULAR: MACH ± BEND ±
TWO PLACE DECIMAL ±
THREE PLACE DECIMAL ±
INTERPRET GEOMETRIC
TOLERANCING PER:
MATERIAL
Plexiglass
FINISH
DO NOT SCALE DRAWING
DRAWN
CHECKED
ENG APPR.
MFG APPR.
QA
COMMENTS:
Include gasket &
respace/resize
fasteners as needed
NAME
RHR
DATE
9/23/13
APPLICATION
USED ON
NEXT ASSY
TITLE:
Container Bottom
KFPL
SIZE
A
DWG. NO.
REV
2
SCALE: 1:3
WEIGHT:
SHEET 1 OF 1
SolidWorks Educational Edition:
For Instructional Use Only.

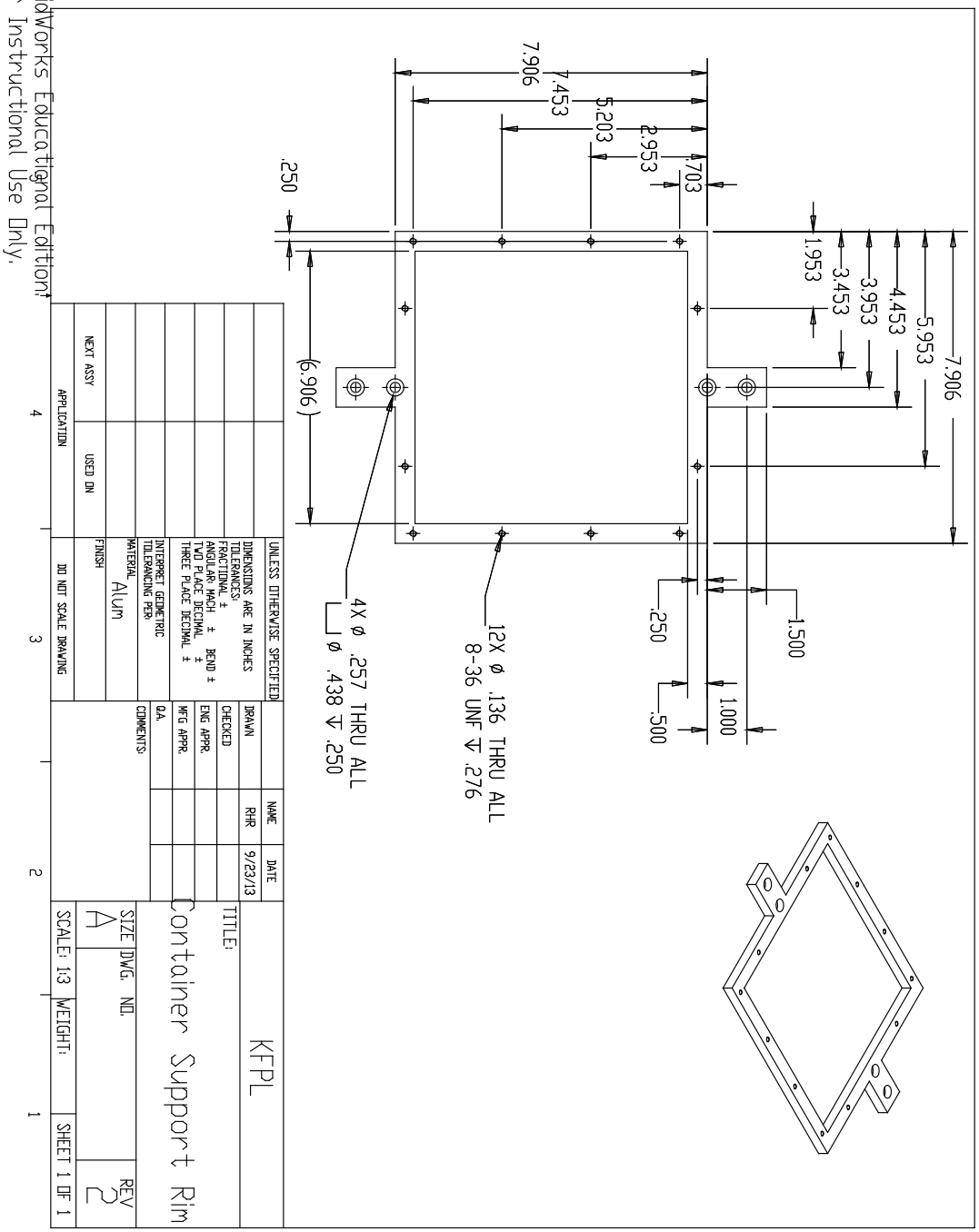
7.906
5.953
4.453
3.953
3.453
1.953
.703
2.953
5.203
7.453
7.906
.250
(6.906)
4X ø .257 THRU ALL
⌴ ø .438 ↧ .250
12X ø .136 THRU ALL
8-36 UNF ↧ .276
.250
.500
1.000
1.500
SolidWorks Educational Edition:
For Instructional Use Only.
UNLESS OTHERWISE SPECIFIED:
DIMENSIONS ARE IN INCHES
TOLERANCES:
FRACTIONAL ±
ANGULAR: MACH ± BEND ±
TWO PLACE DECIMAL ±
THREE PLACE DECIMAL ±
INTERPRET GEOMETRIC
TOLERANCING PER:
MATERIAL
Alum
FINISH
DO NOT SCALE DRAWING
NAME
DATE
DRAWN
RHR
9/23/13
CHECKED
ENG APPR.
MFG APPR.
Q.A.
COMMENTS:
APPLICATION
USED ON
NEXT ASSY
KFPL
TITLE:
Container Support Rim
SIZE
A
DWG. NO.
REV
2
SCALE: 1:3
WEIGHT:
SHEET 1 OF 1

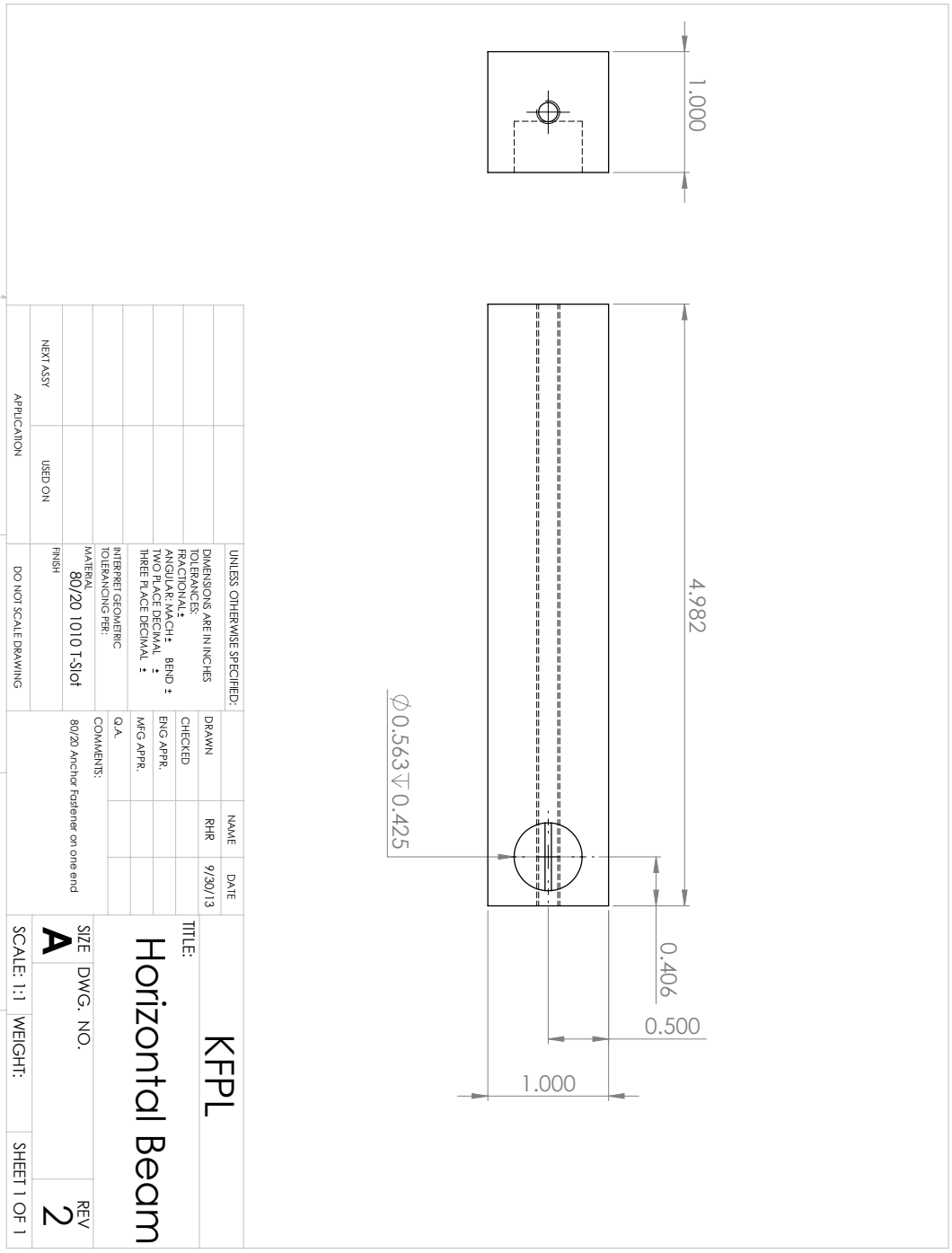
1.000
4.982
∅0.563⩛0.425
0.406
0.500
1.000
UNLESS OTHERWISE SPECIFIED:
DIMENSIONS ARE IN INCHES
TOLERANCES:
FRACTIONAL ±
ANGULAR: MACH ± BEND ±
TWO PLACE DECIMAL ±
THREE PLACE DECIMAL ±
INTERPRET GEOMETRIC TOLERANCING PER:
MATERIAL
80/20 1010 T-Slot
FINISH
DO NOT SCALE DRAWING
APPLICATION
USED ON
NEXT ASSY
DRAWN RHR 9/30/13
CHECKED
ENG APPR.
MFG APPR.
Q.A.
COMMENTS:
80/20 Anchor Fastener on one end
KFPL
TITLE:
Horizontal Beam
SIZE A
DWG. NO.
REV 2
SCALE: 1:1
WEIGHT:
SHEET 1 OF 1

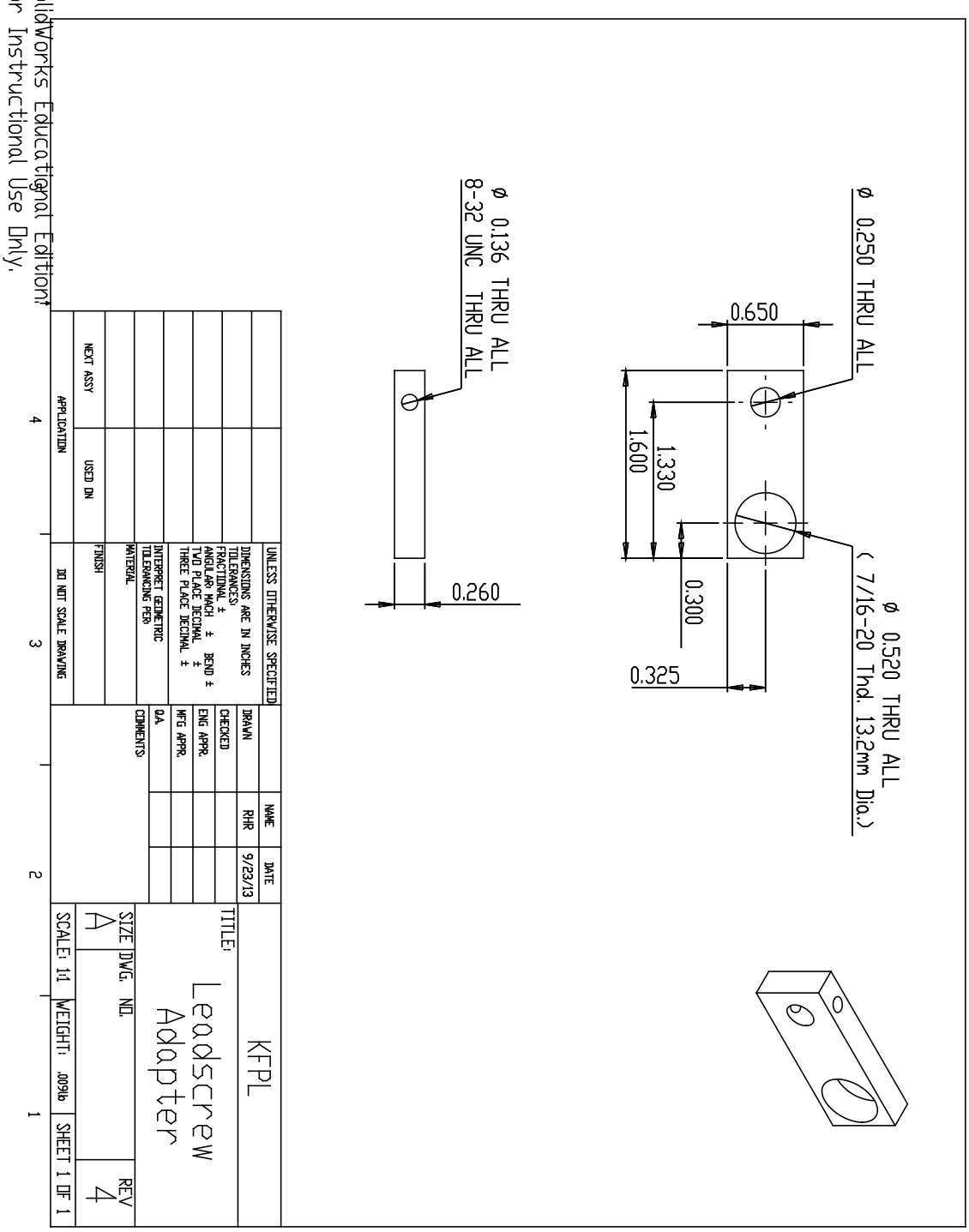
ø 0.250 THRU ALL
ø 0.520 THRU ALL
(7/16-20 Thd. 13.2mm Dia.)
0.650
1.600
1.330
0.300
0.325
ø 0.136 THRU ALL
8-32 UNC THRU ALL
0.260
SolidWorks Educational Edition:
For Instructional Use Only.
UNLESS OTHERWISE SPECIFIED:
DIMENSIONS ARE IN INCHES
TOLERANCES:
FRACTIONAL ±
ANGULAR: MACH ± BEND ±
TWO PLACE DECIMAL ±
THREE PLACE DECIMAL ±
INTERPRET GEOMETRIC TOLERANCING PER:
MATERIAL
FINISH
DO NOT SCALE DRAWING
NAME
DATE
DRAWN
RHR
9/23/13
CHECKED
ENG APPR.
MFG APPR.
Q.A.
COMMENTS:
APPLICATION
USED ON
NEXT ASSY
KFPL
TITLE:
Leadscrew Adapter
SIZE
A
DWG. NO.
REV
4
SCALE: 1:1
WEIGHT: .009lb
SHEET 1 OF 1

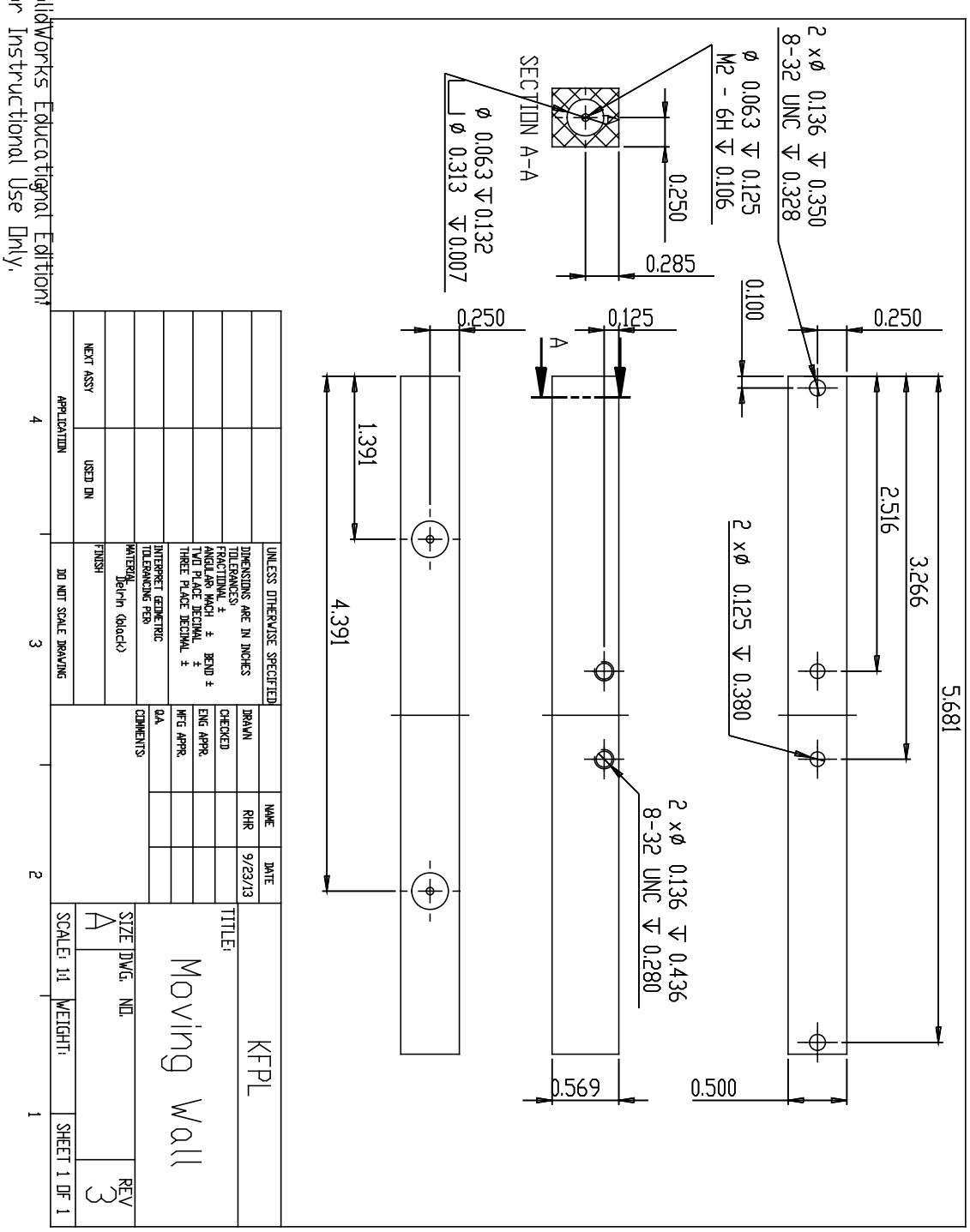
2 x ø 0.136 ↧ 0.350
8-32 UNC ↧ 0.328
ø 0.063 ↧ 0.125
M2 - 6H ↧ 0.106
0.250
0.285
SECTION A-A
ø 0.063 ↧ 0.132
ø 0.313 ↧ 0.007
0.100
0.250
0.125
A
1.391
4.391
5.681
3.266
2.516
2 x ø 0.125 ↧ 0.380
2 x ø 0.136 ↧ 0.436
8-32 UNC ↧ 0.280
0.569
0.500
SolidWorks Educational Edition:
For Instructional Use Only.
UNLESS OTHERWISE SPECIFIED:
DIMENSIONS ARE IN INCHES
TOLERANCES:
FRACTIONAL ±
ANGULAR: MACH ± BEND ±
TWO PLACE DECIMAL ±
THREE PLACE DECIMAL ±
INTERPRET GEOMETRIC TOLERANCING PER:
MATERIAL Delrin (black)
FINISH
DO NOT SCALE DRAWING
NAME
DATE
DRAWN
RHR
9/23/13
CHECKED
ENG APPR.
MFG APPR.
Q.A.
COMMENTS:
NEXT ASSY
USED ON
APPLICATION
TITLE:
KFPL
Moving Wall
SIZE
A
DWG. NO.
REV
3
SCALE: 1:1
WEIGHT:
SHEET 1 OF 1

.125
.453
1.453
2.453
7X ø .089 ↧ .526
4-40 UNC ↧ .224
A
A
.125
.375
.250
6.656
6.906
2X ø .096 THRU ALL
⌵ ø .172 X 82°
.500
.500
SECTION A-A
SolidWorks Educational Edition:
For Instructional Use Only.
UNLESS OTHERWISE SPECIFIED:
DIMENSIONS ARE IN INCHES
TOLERANCES:
FRACTIONAL ±
ANGULAR: MACH ± BEND ±
TWO PLACE DECIMAL ±
THREE PLACE DECIMAL ±
INTERPRET GEOMETRIC TOLERANCING PER:
MATERIAL
Delrin/Plexiglass
FINISH
DO NOT SCALE DRAWING
APPLICATION
USED ON
NEXT ASSY
DRAWN
CHECKED
ENG APPR.
MFG APPR.
Q.A.
COMMENTS:
4-40 threaded holes are .25 deep, not thru
NAME
RHR
DATE
9/23/13
KFPL
TITLE:
Parallel Container Wall
SIZE
A
DWG. NO.
REV
2
SCALE: 1:1
WEIGHT:
SHEET 1 OF 1

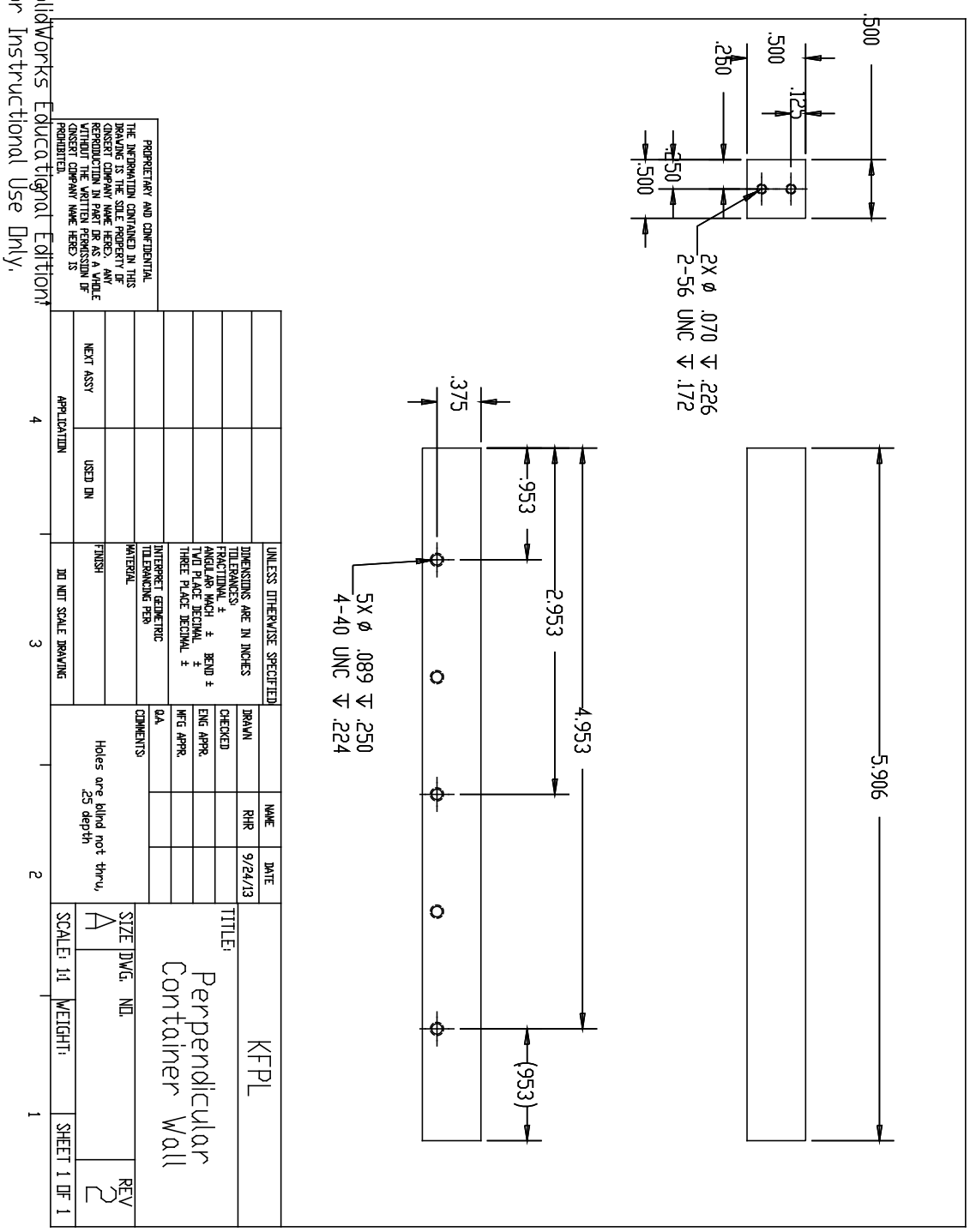
.500
.500
.125
.250
.150
.500
2X ø .070 ↧ .226
2-56 UNC ↧ .172
5.906
.375
.953
2.953
4.953
(.953)
5X ø .089 ↧ .250
4-40 UNC ↧ .224
SolidWorks Educational Edition:
For Instructional Use Only.
PROPRIETARY AND CONFIDENTIAL
THE INFORMATION CONTAINED IN THIS DRAWING IS THE SOLE PROPERTY OF <INSERT COMPANY NAME HERE>. ANY REPRODUCTION IN PART OR AS A WHOLE WITHOUT THE WRITTEN PERMISSION OF <INSERT COMPANY NAME HERE> IS PROHIBITED.
UNLESS OTHERWISE SPECIFIED:
DIMENSIONS ARE IN INCHES
TOLERANCES:
FRACTIONAL ±
ANGULAR: MACH ± BEND ±
TWO PLACE DECIMAL ±
THREE PLACE DECIMAL ±
INTERPRET GEOMETRIC TOLERANCING PER:
MATERIAL
FINISH
DO NOT SCALE DRAWING
NAME
DATE
DRAWN
RHR
9/24/13
CHECKED
ENG APPR.
MFG APPR.
QA
COMMENTS:
Holes are blind not thru, .25 depth
APPLICATION
USED ON
NEXT ASSY
KFPL
TITLE:
Perpendicular Container Wall
SIZE
A
DWG. NO.
REV
2
SCALE: 1:1
WEIGHT:
SHEET 1 OF 1
4
3
2
1

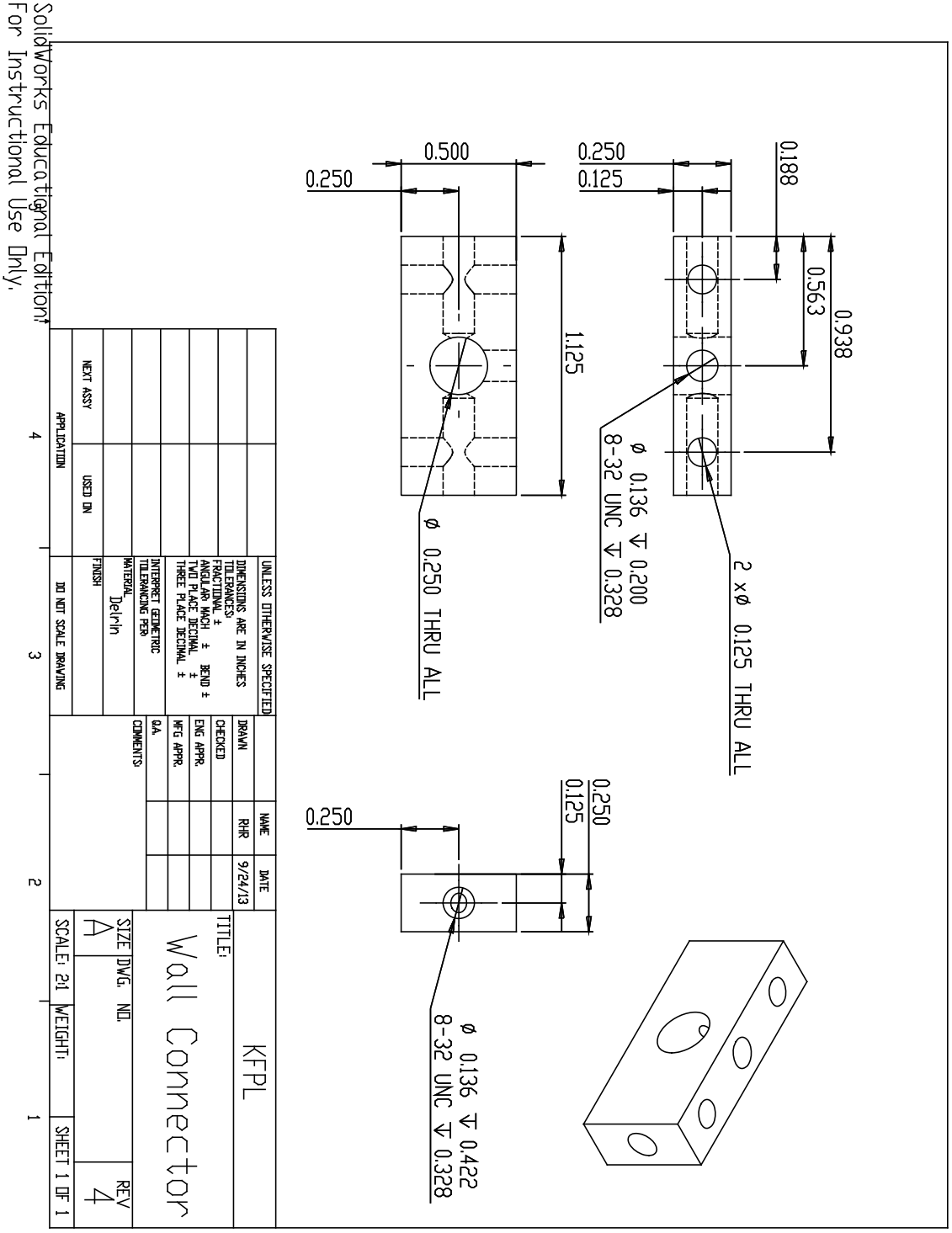
0.188
0.563
0.938
0.250
0.125
0.500
0.250
1.125
ø 0.136 ↧ 0.200
8-32 UNC ↧ 0.328
2 xø 0.125 THRU ALL
ø 0.250 THRU ALL
0.250
0.125
0.250
ø 0.136 ↧ 0.422
8-32 UNC ↧ 0.328
SolidWorks Educational Edition:
For Instructional Use Only.
UNLESS OTHERWISE SPECIFIED:
DIMENSIONS ARE IN INCHES
TOLERANCES:
FRACTIONAL ±
ANGULAR: MACH ± BEND ±
TWO PLACE DECIMAL ±
THREE PLACE DECIMAL ±
INTERPRET GEOMETRIC TOLERANCING PER:
MATERIAL
Delrin
FINISH
DO NOT SCALE DRAWING
NAME
DATE
DRAWN
RHR
9/24/13
CHECKED
ENG APPR.
MFG APPR.
Q.A.
COMMENTS:
NEXT ASSY
USED ON
APPLICATION
TITLE:
Wall Connector
KFPL
SIZE
A
DWG. NO.
REV
4
SCALE: 2:1
WEIGHT:
SHEET 1 OF 1

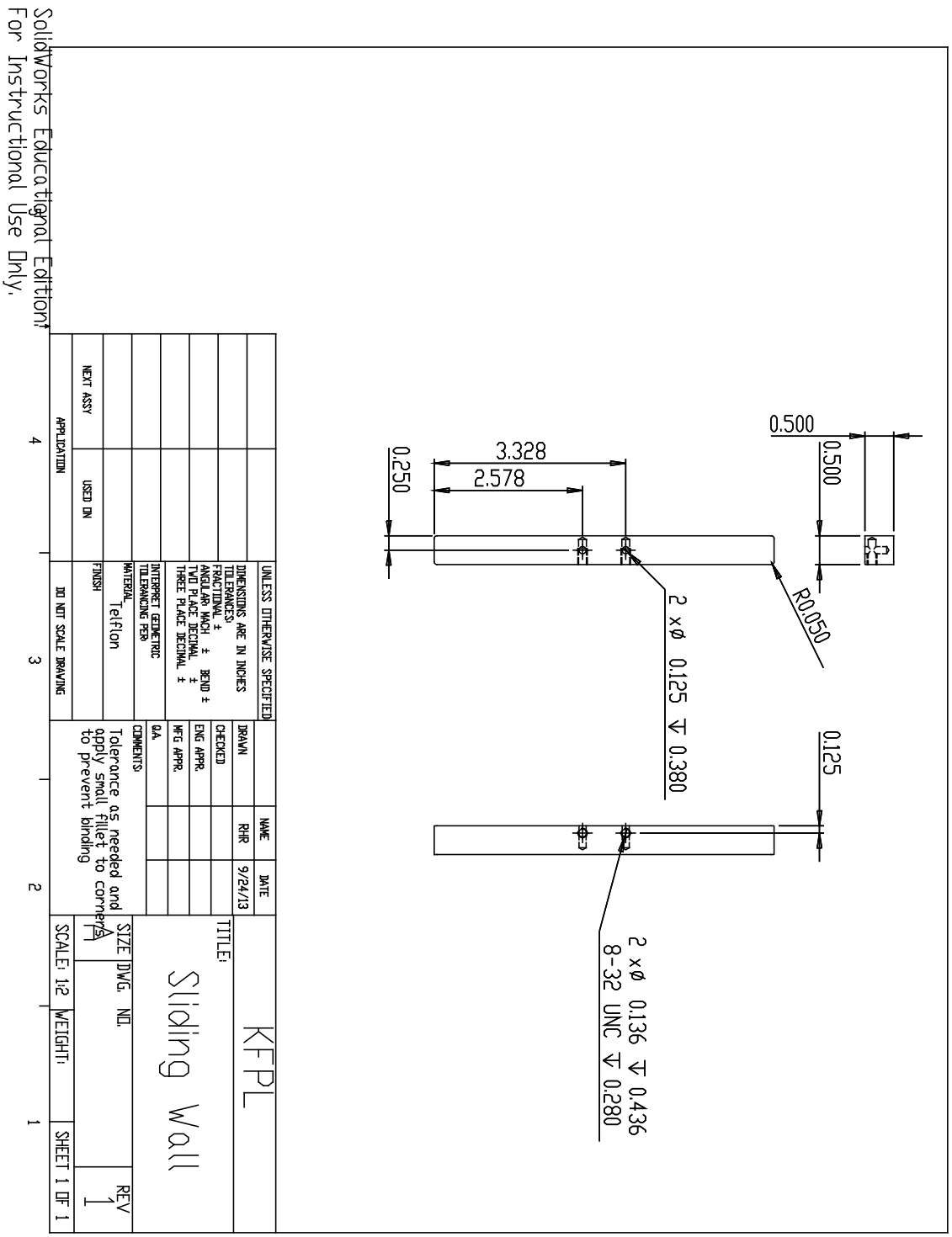
0.500
0.500
3.328
2.578
0.250
R0.050
2 x ø 0.125 ↧ 0.380
0.125
2 x ø 0.136 ↧ 0.436
8-32 UNC ↧ 0.280
UNLESS OTHERWISE SPECIFIED:
DIMENSIONS ARE IN INCHES
TOLERANCES:
FRACTIONAL ±
ANGULAR: MACH ± BEND ±
TWO PLACE DECIMAL ±
THREE PLACE DECIMAL ±
INTERPRET GEOMETRIC TOLERANCING PER:
MATERIAL Teflon
FINISH
DO NOT SCALE DRAWING
NAME
DATE
DRAWN RHR 9/24/13
CHECKED
ENG APPR.
MFG APPR.
QA
COMMENTS:
Tolerance as needed and apply small fillet to corners to prevent binding
APPLICATION
USED ON
NEXT ASSY
KFPL
TITLE:
Sliding Wall
SIZE A
DWG. NO.
REV 1
SCALE: 1:2
WEIGHT:
SHEET 1 OF 1
SolidWorks Educational Edition:
For Instructional Use Only.

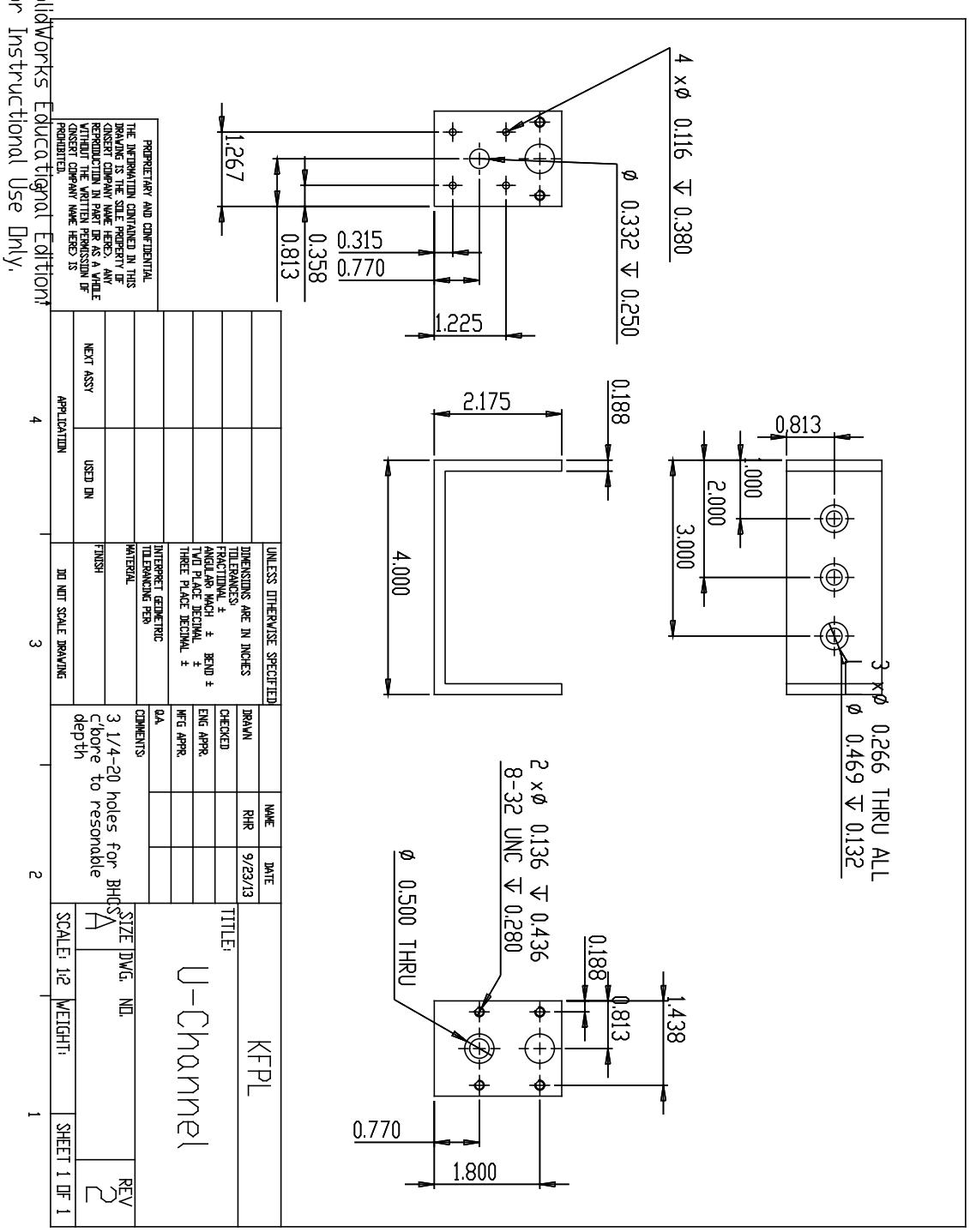
4 xø 0.116 ↧ 0.380
ø 0.332 ↧ 0.250
1.267
0.813
0.358
0.315
0.770
1.225
2.175
0.188
4.000
0.813
1.000
2.000
3.000
3 xø 0.266 THRU ALL
ø 0.469 ↧ 0.132
2 xø 0.136 ↧ 0.436
8-32 UNC ↧ 0.280
ø 0.500 THRU
0.188
0.813
1.438
0.770
1.800
SolidWorks Educational Edition:
For Instructional Use Only.
PROPRIETARY AND CONFIDENTIAL
THE INFORMATION CONTAINED IN THIS DRAWING IS THE SOLE PROPERTY OF <INSERT COMPANY NAME HERE>. ANY REPRODUCTION IN PART OR AS A WHOLE WITHOUT THE WRITTEN PERMISSION OF <INSERT COMPANY NAME HERE> IS PROHIBITED.
UNLESS OTHERWISE SPECIFIED:
DIMENSIONS ARE IN INCHES
TOLERANCES:
FRACTIONAL ±
ANGULAR: MACH ± BEND ±
TWO PLACE DECIMAL ±
THREE PLACE DECIMAL ±
INTERPRET GEOMETRIC TOLERANCING PER:
MATERIAL
FINISH
DO NOT SCALE DRAWING
NAME
DATE
DRAWN
RHR
9/23/13
CHECKED
ENG APPR.
MFG APPR.
Q.A.
COMMENTS:
3 1/4-20 holes for BHCS c'bore to resonable depth
APPLICATION
NEXT ASSY
USED ON
TITLE:
U-Channel
KFPL
SIZE
A
DWG. NO.
REV
2
SCALE: 1:2
WEIGHT:
SHEET 1 OF 1
4
3
2
1

ø 0.252
[6.40]
THD THRU ALL
ø 0.313
0.38
INNER THREAD: Mates with
6.4mm screw dia.
PTFE coated leadscrew
3mm lead (3mm/1rev)
UNLESS OTHERWISE SPECIFIED:
DIMENSIONS ARE IN INCHES
TOLERANCES:
FRACTIONAL ±
ANGULAR: MACH ± BEND ±
TWO PLACE DECIMAL ±
THREE PLACE DECIMAL ±
INTERPRET GEOMETRIC TOLERANCING PER:
MATERIAL
Delrin or similar
FINISH
DO NOT SCALE DRAWING
DRAWN
CHECKED
ENG APPR.
MFG APPR.
QA
COMMENTS:
QTY: 2
NAME
DATE
RHR
12/16/2013
TITLE:
Threaded Standoff
KFPL
SIZE
A
DWG. NO.
REV
1
SCALE: 5:1
WEIGHT:
SHEET 1 OF 1
NEXT ASSY
USED ON
APPLICATION
PROPRIETARY AND CONFIDENTIAL
THE INFORMATION CONTAINED IN THIS DRAWING IS THE SOLE PROPERTY OF <INSERT COMPANY NAME HERE>. ANY REPRODUCTION IN PART OR AS A WHOLE WITHOUT THE WRITTEN PERMISSION OF <INSERT COMPANY NAME HERE> IS PROHIBITED.
SolidWorks Educational Edition
For Instructional Use Only.
4
3
2
1

1.000
1.000
ø 0.201 THRU ALL
1/4-20 UNC THRU ALL
8.000
SolidWorks Educational Edition:
For Instructional Use Only.
UNLESS OTHERWISE SPECIFIED:
DIMENSIONS ARE IN INCHES
TOLERANCES:
FRACTIONAL ±
ANGULAR: MACH ± BEND ±
TWO PLACE DECIMAL ±
THREE PLACE DECIMAL ±
INTERPRET GEOMETRIC TOLERANCING PER:
MATERIAL
1010 T-Slot
FINISH
DO NOT SCALE DRAWING
NAME
DATE
DRAWN
RHR
10/1/13
CHECKED
ENG APPR.
MFG APPR.
Q.A.
COMMENTS:
More important that absolute length is that both pairs of beams be closely matched
KFPL
TITLE:
Vertical Beam
SIZE
A
DWG. NO.
REV
SCALE: 1:2
WEIGHT:
SHEET 1 OF 1
APPLICATION
NEXT ASSY
USED ON

Appendix C

Software programs

C.1 EASI-V code for controllers

Below is the SETUP2.PRG file which operates the ViX drive.

```
1  ;*********************************************************
2  ; Example setup program for ViX-IM drive
3  ; Generated by Easi-V
4  ;*********************************************************
5  ; Notes:
6  ; 1) Prefix ALL commands with an axis address number
7  ; 2) Spaces are not allowed in any command e.g. 2GOSUB (FRED
       )
8  ;    is a syntax error
9  ; 3) A semi-colon (;) denotes the start of a comment
10 ; 4) Comments are not stored in the drive
11 ; 5) CLEAR all routines before re-defining them
12 ; 6) DECLARE user-defined labels before use
13 ; 7) Define a PROFILE before USEing it
14 ;*********************************************************
15 0K                      ;Kill any program that is running
16 0CLEAR(ALL)             ;Erase all routines, etc
17
18 0START:                 ;Define power-up START routine
19   0DECLARE(MOVE)        ;Declare routine 'MOVE'
20   0DECLARE(INIT)        ;Declare routine 'INIT'
21
```

```
22   0ON                    ;Enable motor
23   0O(000)                ;Outputs off
24
25   0PROFILE1(1,1,250000,.33)     ;Move profile 1
26   0USE(1)                ;Use profile 1
27   0LOOP(MOVE,10)         ;Call 'MOVE' routine 10 times
28 0END                     ;End of routine
29
30 0INIT:                   ;Define INIT routine
31   0OFF          ;Disable motor
32
33   0W(AO,0)               ;Analogue offset
34   0W(AB,0)               ;Deadband
35
36   0W(EX,3)               ;Communications settings
37   0W(EQ,0)               ;Echo queueing
38   0W(BR,9600)    ;BAUD rate
39
40   0W(CQ,1)               ;Command queueing
41
42   0W(IC,8160)    ;I/O configuration
43   0W(EI,2)               ;Following encoder inputs
44   0W(EO,2)               ;Simulated encoder outputs
45   0LIMITS(3,1,0,200.00) ;Travel limits
46
47   0W(IT,10)              ;Settling time
48
49   0W(ES,1)               ;Drive enable sense (can over-ride
        input)
50
51   ;Motor configuration
52   0MOTOR(201,0.5,50000,1000,4,2.80,3.40)
53 0W(MS,50)                ;% current standby reduction
54
55 0END                     ;End of routine
56
57 0MOVE:           ;Define 'MOVE' routine
58   0O(1)          ;Output1 on
59   0G                     ;Do move
60   0O(0)          ;Output1 off
61   ;0T1                   ;Wait
62   0H                     ;Switch direction
```

```
63 0END                    ;End of routine
64
65 0ARM00                  ;No auto-run on power-up
66 0GOTO(INIT)             ;Execute INIT routine
67
68 ;Ensure you save changes (SV) and reset the drive (Z) AFTER
      the GOTO(INIT)
69 ;If auto-run of START routine is not enabled (ARM1x), type
      in:
70 ;0GOTO(START) in the TERMINAL window to run START
```

C.2 MATLAB Code

Below is the MATLAB script or code im_analyze5_2.m which analyzes the images and outputs the surface topography of the given images.

```
1  function im_analyze5_2()
2  % im_analyze5_2.m
3  % Generates a movie output
4  % -------------- Program Variables
      ---------------------------------%
5  im_dir = 'trial_32_8_3\';   % Folder where images or video
      are stored
6  % im_dir = 'Trial 30_1\';     % Folder where images or video
       are stored
7  % im_dir = 'Nov 6\';
8  % im_list = 'All';          % Images or frames to read. 1st
      image sets reference plane
9  % im_list = [1:3, 46:51];     % Trial 32_8_2
10 im_list = [55:91];     % Trial 32_8_3
11 % im_list = [1:4, 160:169];   % For Trial 30_1
12 plots_on = 1;                  % Generate diagnostic plots
13
14 % ----------- Experimental Parameters
      -----------------------------%
15 L_0 = (28+4)*25.4;      % Distance from object to camera &
      projector: mm
```

```
16 D = 4.75*25.4;              % Distance from camera to
      projector: mm
17 % f_0 = 13.5/25.4;         % Fundamental frequency of
      observed grating, gratings/mm
18 % pixel_pitch = 190/25.4;        % pixels / mm
19 pixel_pitch = 6.59;          % Trial 30 -- pixels / mm
20 % win_length = 40;         % = 1/standard deviation: pixels
      ^-1
21
22
23 % -------- Data analysis variables
      ------------------------------%
24 ROI = [1, 1, 1280, 1024];     % Trial 32_8
25 % ROI = [210, 40, 1150, 750];   % X Start (1st column), Y
      start (1st row),
26 % %                              % X End (last column), Y end
       (last row)
27 % ROI = 'off';
28 rotate_on = 0;      % 0 if gratings are horizontal (default)
      , 1 rotates images
29 high_pass_wid = 90;          % Width of high pass gaussian
      filter
30 gauss_filter_ratio = 1/10;   % Ratio of standard deviation
      to wavenumber
31 Avg_height = 0;
32
33 % ------------ Read images ------------------------------%
34 files = dir(im_dir);
35 if strcmpi(files(3).name(end-2:end),'avi')
36     if ischar(im_list)
37         im_list = 1:length(files);      % Create a list of
              all frames in video to import
38     end
39
40     num_images = length(im_list);
41     readerobj = mmreader(strcat(im_dir, files(3).name));
42     im.name = readerobj.Name;
43     for i = 1:num_images
44         temp = read(readerobj,im_list(i));  % Read frame
45         im(i).image = temp(:,:,1);      % for B&W images
              only use R of RGB
46     end
```

```
47 else
48     if ischar(im_list)
49         im_list = 1:(length(files)-2);  % Create a list of
               all images in directory
50     end
51     num_images = length(im_list);
52     for i = 1:num_images
53         im(i).image = imread(strcat(im_dir, files(im_list(i)
               +2).name));
54         im(i).name = files(im_list(i)+2).name;
55     end
56
57 end
58
59 % ------------- Region of Interest ------------------------%
60 if plots_on >= 1
61     subplot(1,2,1)
62     imshow(im(1).image, [0 mean(max(im(1).image))])
63     title('Reference image')
64 end
65 if ~ischar(ROI(1))
66     if plots_on
67         hold on
68         plot([ROI(1),ROI(3),ROI(3),ROI(1),ROI(1)],[ROI(2),
               ROI(2),...
69             ROI(4),ROI(4),ROI(2)], 'Color','red', 'LineWidth
                   ',1)  % Rectangle over ROI
70         hold off
71     end
72
73     % Discard subset of image not in ROI
74     for i = 1:num_images
75         im(i).image = im(i).image(ROI(2):ROI(4),ROI(1):ROI
               (3));
76     end
77 end
78
79 if rotate_on
80     for i = 1:num_images
81         im(i).image = im(i).image';
82     end
83 end
```

```
84
85
86 % ----------- Analysis & processing
      ------------------------%
87 [N c] = size(im(1).image);      % N is the length of the
      column vectors = fft length
88 % NFFT = 2^nextpow2(N);           % Next power of 2
89 mid_x = floor(c/2);
90 mid_y = floor(N/2);
91 x_p = 0:c-1;                     % X Pixels
92 y_p = 0:N-1;                     % Y Pixels
93
94 y_range = floor(.45*N:.55*N);
95 mich_contrast = double(max(im(1).image(y_range,mid_x)) - min
      (im(1).image(y_range,mid_x)))...
96     / double(max(im(1).image(y_range,mid_x)) + min(im(1).
         image(y_range,mid_x)));
97
98
99 if plots_on >= 1
100     subplot(1,2,1)
101     hold on
102     plot([ROI(1)+mid_x,ROI(1)+mid_x],[ROI(2)+y_range(1),ROI
         (2)+y_range(end)],...
103         'Color','blue', 'LineWidth',1);
104     hold off
105
106     subplot(1,2,2);
107     plot(y_range,im(1).image(y_range,mid_x))
108         title(sprintf('Michelson Contrast = %1.2f',
               mich_contrast))
109     xlabel('Y (pixels)')
110     ylabel('Intensity')
111 %     xlim([1 2])
112 end
113
114 % % Remove average
115 % im_1 = im_1 - mean(mean(im_1));
116 % im_2 = im_2 - mean(mean(im_2));
117
118 % ---------- Take Fourier Transform -----------
```

```
119 filt = fspecial('disk',3);      % Initialize averaging
       filter
120
121 for i = 1:num_images
122 %       im(i).image = imfilter(im(i).image, filt);  % Filter
        image first
123     im(i).fft = fft(imfilter(double(im(i).image),filt));
124 %     im(i).image = fft(im(i).image);       % Fourier
       transform columns
125 end
126
127
128 % --------- Plot power spectrum ---------------
129 f0 = (-N/2:N/2-1);
130
131 % % Plot single-sided amplitude spectrum.
132 % f = 1/2*linspace(0,1,NFFT/2+1);
133 % plot(f,2*abs(im(1).fft(1:NFFT/2+1,mid_x)))
134 % title('Single-Sided Amplitude Spectrum of y(t)')
135 % xlabel('Frequency (Hz)')
136 % ylabel('|Y(f)|')
137
138 if plots_on >= 3
139     % 2D Plot
140     mesh(x_p,f0,fftshift(abs(im(1).fft)))
141 end
142
143 % ----------- Window (filter) data ------------
144 % High-pass filter (remove lowest frequencies)
145 win = 1-gausswin(N,high_pass_wid);
146 if plots_on >= 2
147     plot(fftshift(abs(im(1).fft(:,mid_x))))
148     hold on
149     plot(win*max(abs(im(1).fft(:,mid_x))))
150     hold off
151 end
152
153 win = repmat(win,1,c);
154 for i = 1:num_images
155     im(i).fft = ifftshift(fftshift(im(i).fft).*win);
156 end
157
```

```
158 % im_1 = ifftshift(fftshift(im_1).*repmat(win,1,c));
159 % im_2 = ifftshift(fftshift(im_2).*repmat(win,1,c));
160
161 % Identify where to filter using reference image (this
       happens once)
162 [C I] = max(abs(im(1).fft(:,mid_x)));
163 % shift_length = I;
164 shift_length = I-round(N/2);
165 win_length = (I-1)*gauss_filter_ratio;       % Standard
       deviation of window
166 win = circshift(gausswin(N,(N/2)/(win_length)),shift_length)
       ; % Generate and shift gaussian window
167 win = win/max(win);
168
169 if plots_on >= 1
170     plot(abs(im(1).fft(:,mid_x))/N)
171     hold on
172     plot(win*max(abs(im(1).fft(:,mid_x)))/N)
173     title(sprintf('Gaussian Filter with Sigma = %1.2f',
           win_length))
174     xlim([0 3*I])
175     hold off
176 end
177
178 win = repmat(win,1,c);      % Apply window to fft data
179 for i = 1:num_images
180     im(i).fft = im(i).fft.*win;
181 end
182 clear win
183
184 % ----- Transform back to real space -------
185 filt = fspecial('disk',13); % Initialize averaging filter
186
187 for i = 1:num_images
188     im(i).phase = ifft(im(i).fft);
189     im(i).fft = [];         % Clear fft to save memory
190     im(i).image = [];       % Clear image as well
191 end
192
193 f_0 = (I/N)*pixel_pitch;        % Gratings / pixel * pixel/
       mm
```

```
194 % ---- Calculate delta_phi (change of phase with respect to
       reference)---
195 for i = 2:num_images
196     im(i).phase = angle(im(i).phase.*conj(im(1).phase));
197
198     im(i).phase = imfilter(im(i).phase, filt); % Image
           filter
199
200     im(i).phase = unwrap(im(i).phase);      % Remove jumps
           along columns
201     im(i).phase = unwrap(im(i).phase')';    % Check for
           jumps along rows too
202
203     im(i).h = L_0 * im(i).phase./(im(i).phase-2*pi*f_0*D); %
           Compute height from phase
204     im(i).phase = [];                       % Clear phase
           data to save memory
205
206     if rotate_on==1
207         im(i).h = im(i).h';  % flip back to original
               orientation
208     end
209
210     Avg_height(i) = mean(mean(im(i).h));
211     ind = find(abs(im(i).h - Avg_height(i)) > 4* mean(std(im
           (i).h)));   % Toss out extreme, spurious points
212     im(i).h(ind) = Avg_height(i);       % Replace spurious
           points with avg height
213
214 % %     figure(1)
215 %     mesh(x_p/pixel_pitch, y_p/pixel_pitch, im(i).h)
216 %     if i == 2
217 %     title(sprintf('Image %g of %g', i-1, num_images-1))
218 %     xlabel('X (mm)')
219 %     ylabel('Y (mm)')
220 %     zlabel('Z (mm)')
221 %     zlim([-2 2])
222 % %     axis tight
223 %     set(gca,'nextplot','replacechildren');
224 %     end
225 %     F(i-1) = getframe;
226
```

```
227 %     figure(2)
228 %
229 %     subplot(2,2,1)
230 %     plot(f0,fftshift(abs(im(i).fft(:,mid_x))))
231 %     title('Filtered Frequency')
232 %     subplot(2,2,2)
233 %     plot(y_p,im(i).phase(:,mid_x))
234 %     title('Unwrapped Phase')
235 %     ylabel('Radians')
236 %     subplot(2,2,3)
237 %     plot(y_p/pixel_pitch,im(i).h(:,mid_x))
238 %       title('Middle X Slice')
239 %     xlabel('Y (mm)')
240 %     subplot(2,2,4)
241 %       plot(x_p/pixel_pitch,im(i).h(mid_y,:))
242 %     title('Middle Y')
243 %     ylabel('Height (mm)')
244 %     xlabel('X (mm)')
245 end
246
247 mesh(x_p/pixel_pitch, y_p/pixel_pitch, im(2).h)
248 title(sprintf('Image %g of %g', 1, num_images-1))
249 xlabel('X (mm)')
250 ylabel('Y (mm)')
251 zlabel('Z (mm)')
252 zlim([-1 1])
253
254 % set(gca,'nextplot','replacechildren');
255 drawnow
256 pause(1)
257 F(1) = getframe(gcf);
258 [X,Map] = frame2im(F(1));
259
260 for i = 3:num_images
261
262     mesh(x_p/pixel_pitch, y_p/pixel_pitch, im(i).h)
263     title(sprintf('Image %g of %g', i-1, num_images-1))
264     xlabel('X (mm)')
265     ylabel('Y (mm)'), zlabel('Z (mm)'), zlim([-1 1])
266     drawnow
267     pause(.5)
268     F(i-1) = getframe(gcf);
```

```
269     [X(:,:,:,i-1),Map(:,:,:,i-1)] = frame2im(F(i-1));
270 end
271
272 % h2 = figure;
273 % movie(h2, F,2,1)
274
275 % ---- Make a Movie ------
276 mov = immovie(X,Map);
277 movie2avi(mov,'test6','fps',1)
278 % zlim([0 .3])
279 % figure
280 % plot(y_p/pixel_pitch,im.h(mid_x,:))
281 end
```